MOLECULAR AND CELLULAR BIOLOGY, Apr. 2006, p. 3266–3281 Vol. 26, No. 8
0270-7306/06/$08.00+0 doi:10.1128/MCB.26.8.3266–3281.2006

Differentiation of Trophoblast Giant Cells and Their Metabolic Functions Are Dependent on Peroxisome Proliferator-Activated Receptor β/δ

Karim Nadra,[1] Silvia I. Anghel,[1,2] Elisabeth Joye,[1] Nguan Soon Tan,[1]† Sharmila Basu-Modak,[1]‡ Didier Trono,[2,3] Walter Wahli,[1,2] and Béatrice Desvergne[1,2]*

Center for Integrative Genomics, University of Lausanne, CH-1015 Lausanne, Switzerland[1]; National Research Center "Frontiers in Genetics"[2]§; and School of Life Sciences, Swiss Federal Institute of Technology, Lausanne, Switzerland[3]

Received 24 June 2005/Returned for modification 21 July 2005/Accepted 24 January 2006

Mutation of the nuclear receptor peroxisome proliferator-activated receptor β/δ (PPARβ/δ) severely affects placenta development, leading to embryonic death at embryonic day 9.5 (E9.5) to E10.5 of most, but not all, PPARβ/δ-null mutant embryos. While very little is known at present about the pathway governed by PPARβ/δ in the developing placenta, this paper demonstrates that the main alteration of the placenta of PPARβ/δ-null embryos is found in the giant cell layer. PPARβ/δ activity is in fact essential for the differentiation of the Rcho-1 cells in giant cells, as shown by the severe inhibition of differentiation once PPARβ/δ is silenced. Conversely, exposure of Rcho-1 cells to a PPARβ/δ agonist triggers a massive differentiation via increased expression of 3-phosphoinositide-dependent kinase 1 and integrin-linked kinase and subsequent phosphorylation of Akt. The links between PPARβ/δ activity in giant cells and its role on Akt activity are further strengthened by the remarkable pattern of phospho-Akt expression in vivo at E9.5, specifically in the nucleus of the giant cells. In addition to this phosphatidylinositol 3-kinase/Akt main pathway, PPARβ/δ also induced giant cell differentiation via increased expression of I-mfa, an inhibitor of Mash-2 activity. Finally, giant cell differentiation at E9.5 is accompanied by a PPARβ/δ-dependent accumulation of lipid droplets and an increased expression of the adipose differentiation-related protein (also called adipophilin), which may participate to lipid metabolism and/or steroidogenesis. Altogether, this important role of PPARβ/δ in placenta development and giant cell differentiation should be considered when contemplating the potency of PPARβ/δ agonist as therapeutic agents of broad application.

The earliest cell differentiation event in the mammalian embryo is the formation of the trophectoderm, which consists of two regions: the polar trophectoderm, directly adjacent to the inner cell mass, and the mural trophectoderm surrounding the blastocoelic cavity. In rodent placentas, the cells of the mural trophectoderm differentiate into a limited number of nondividing primary giant cells during implantation, whereas those of the polar trophectoderm proliferate to form the ectoplacental cone and develop a multitude of secondary giant cells (20).

Trophoblast giant cells participate in a number of processes essential to a successful pregnancy, including blastocyst implantation, remodeling of the maternal deciduas, and secretion of hormones that regulate the development of both the fetal and maternal compartments of the placenta. In the early stages, the inherent invasive properties of these cells appear to be crucial for remodeling in the maternal uterine stroma. At later stages, after embryonic day 9.5 (E9.5), the secondary giant cells produce a number of placental hormones, particularly members of the prolactin/growth hormone family of proteins, which in mice includes placental lactogen I (PL-I), PL-II, and proliferin (49). The expression of these trophoblast giant cell functions coincides with a very critical period of placental development, exemplified by the high incidence of embryonic lethality at that stage. Paradoxically, very little is yet known about the giant cell differentiation process.

Peroxisome proliferator-activated receptors (PPARs) are lipid-activated transcription factors that belong to the nuclear hormone receptor family. Three isotypes of PPARs have been cloned: PPARα (NR1C1; Nuclear Receptor Nomenclature Committee 1999), PPARβ/δ (NR1C2; also called NUC-1 or FAAR and which will be hereafter referred to as PPARβ), and PPARγ (NR1C3), all of which bind to DNA as heterodimers with retinoid X receptor (RXR; NR2B) (10). While PPARα and PPARγ have clearly defined roles in controlling lipid and glucose homeostasis (64), various physiological roles of PPARβ are still being investigated. PPARβ has been linked to embryo implantation (41, 42), myelination in the brain (51), osteoclastic bone resorption (44), and skin wound healing (46, 58). Its role in lipid metabolism comprises diverse facets associated with the preadipocyte clonal expansion (26, 29), fatty acid oxidation in muscle (63), or lipoprotein homeostasis (50). The nature of the endogenous PPARβ ligands remains to be ascertained. Similar to the other two PPARs, some polyunsaturated fatty acids have affinities for PPARβ in the low micromolar range. More specifically, a number of eicosanoids, particularly prostacyclin, which is a cyclooxygenase 2 arachidonate metabolite, was shown to activate PPARβ (16, 35, 37).

* Corresponding author. Mailing address: Center for Integrative Genomics, University of Lausanne, CH-1015 Lausanne, Switzerland. Phone: 41 21 6924140. Fax: 41 21 6924115. E-mail: beatrice.desvergne@unil.ch.

† Present address: School of Biological Sciences, Nanyang Technological University, 60 Nanyang Drive, Singapore 637551, Singapore.

‡ Present address: Department of Zoology, University of Dehli, Dehli 110007, India.

§ http://www.frontiers-in-genetics.org/en/index.php.

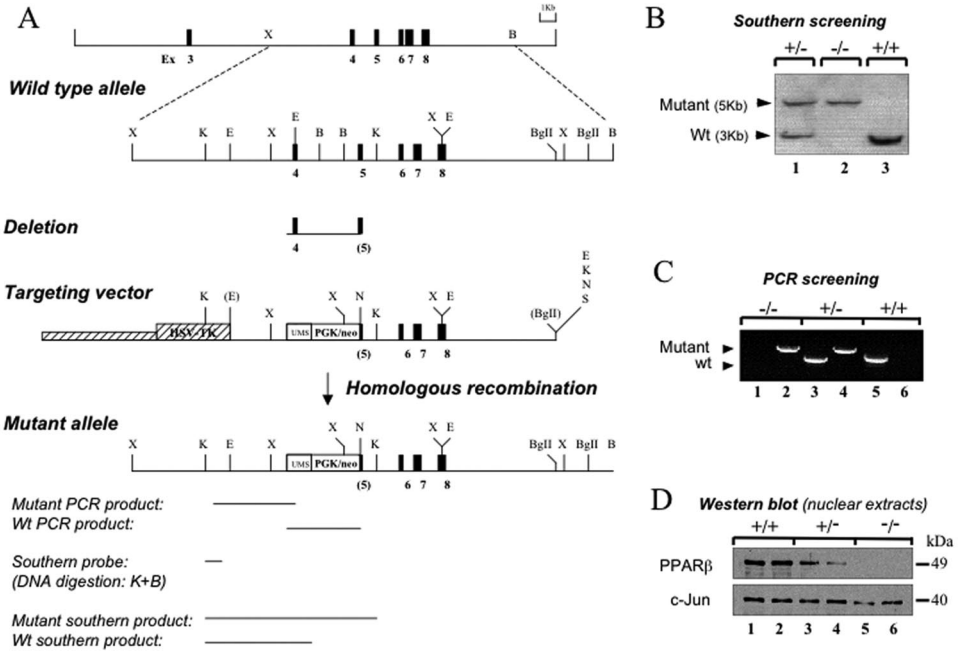

FIG. 1. Targeted disruption of the PPARβ gene in mouse. The PPARβ gene was disrupted in ES cells by homologous recombination with a replacement-type vector, using an approach based on positive-negative selection (A). In this vector, PPARβ genomic sequences containing the exons encoding the DNA-binding domain of the receptor (exon 4 and part of exon 5) were replaced with a PGK-neo cassette. Homologous recombination at the PPARβ locus in ES cells led to the deletion of both exon 4 and part of exon 5 encoding the two zinc fingers of the DNA-binding domain. ES cells carrying the mutant allele were confirmed by Southern blot analysis (B). Two independent positive ES cell clones were injected into blastocysts to generate chimeras, and heterozygous mice were obtained from a germ line transmitter chimera. Panel A shows the structure of the wt PPARβ allele, targeting vector, and recombinant PPARβ allele. The exons as well as locations of restriction sites and probes for PCR and southern blot are indicated. B, BamHI; E, EcoRI; K, KpnI; N, NotI; X, XhoI. Panel B shows a Southern blot analysis of genomic DNA digested with BamHI and KpnI from E9.5 embryos produced by a PPARβ heterozygous intercross. (C) PCR analysis of yolk sac DNA derived from E9.5 embryos. (D) Western blot analysis performed on nuclear extracts with a specific PPARβ antibody. The nuclear protein c-Jun was used as an internal control. In order to obtain a sufficient amount of material, the control at the protein level was performed on pups obtained from homozygous matings.

A crucial tool for understanding PPAR functions in an in vivo and physiological context is the generation of strains of mice carrying mutations in the PPAR genes. However, most of the PPARβ and all PPARγ null embryos die at an early developmental stage because of placental defects (1, 2, 38) that have so far been poorly characterized. In the present work, we delineate a pivotal role of PPARβ in the early events of placental development. Whereas deficiency of PPARγ leads to impaired vascularization (1, 38), deletion of the PPARβ gene causes a severe failure of the placenta to undergo proper morphogenesis, leading to embryonic lethality at E9.5 to E10.5. The trophoblast giant cell layer is the most affected, and we demonstrate a direct involvement of PPARβ in promoting trophoblast cell differentiation toward giant cells. This effect is dependent on phosphatidylinositol 3-kinase (PI3K) and Akt1 (also called protein kinase B) and is at least partly due to the high expression levels of two kinases involved in Akt activation, namely 3-phosphoinositide-dependent kinase 1 (PDK1) and integrin-linked kinase (ILK). In addition, PPARβ caused increased expression of a non-helix-loop-helix (non-HLH) inhibitor of the myogenic basic HLH (bHLH) subfamily, I-mfa (7), which contributes to the differentiation process. Finally, we reveal that giant cells are the primary sites of lipid accumulation in the placenta at an early stage, together with a PPARβ-dependent up-regulation of adipose differentiation-related protein (ADRP) expression. Taken together, these cellular and in vivo approaches unveil important new aspects of the development and functions of the giant cell layer, which has a major impact on placenta development.

MATERIALS AND METHODS

Targeted disruption of the mouse PPARβ. (i) Construction of a replacement vector for PPARβ. Nine overlapping mouse PPARβ genomic clones were isolated from an Sv129 mouse embryonic stem (ES) cell genomic library (gift from F. Conquet), and their restriction maps were established (Fig. 1). A targeting vector was designed to delete the two exons encoding the DNA binding domain (i.e., exons 4 and 5), according to the organization of the *Xenopus* PPARβ gene. The targeting vector (derived from TK-NEO-UMS, a vector comprised of the thymidine kinase gene, neomycin resistance sequence, and upstream mouse sequence; a gift from Charles Weissman [54]) contained 1.7 kb of homologous sequence at the 5′ end, 7 kb of homologous sequence at the 3′ end, and a phosphoglycerate kinase-neomycin (PGK-neo) cassette (Fig. 1A).

(ii) ES cell transfection. D3 ES cells (13) were cultured as previously described (22), and electroporation was performed as previously reported (59). Twenty-four hours after electroporation, positive selection by G418 at 350 μg/ml (geneticin) was performed for 9 days. Resistant clones were then transferred onto 48-well plates (Costar) and subsequently grown to confluence on duplicate 24-well plates for either genomic analysis or storage of master plates at −80°C.

(iii) Genotyping. Genomic DNA was prepared from ES cells, yolk sacs of embryos, or tail samples following the classical procedures. A first round of genotyping was performed by two independent PCRs. Primers b19 (5′-ATCCA GAGTGTTCGTATGAC-3′) and UMS1 (5′-TCTTATGCTCCTGAAGTCCA C-3′) amplified a 2.2-kb fragment from the recombinant allele, whereas the

primers b3 (5′-AGCCTCAACATGGAATGTCG-3′) and b4 (5′-GATCGCAC TTCTCATACTCG-3′) amplified a 1.6-kb product from the wild-type (wt) allele. Five percent of the neomycin-resistant ES cell clones were positive for homologous recombination. All mutant clones and/or embryos or mice were subsequently confirmed by Southern analyses using a digoxigenin-labeled probe (CDP-Star protocol; Boehringer Mannheim), located 160 bp upstream of the 5′ homology region. Digested genomic DNA samples were blotted on a Zetaprobe GT membrane and processed following the manufacturer's protocol (Bio-Rad). Probes, restriction digestion, and hybridized fragments from wt and recombinant alleles are indicated in Fig. 1.

(iv) Generation of chimeric mice and germ line transmission. Positive D3 clones were microinjected into the blastocoel of 3.5-day-old embryos at the blastocyst stage and isolated from C57BL/6 females (10 to 15 ES cells per blastocyst). Between five and seven injected blastocysts were reimplanted into each uterine horn of pseudopregnant foster mothers. Male chimeric animals were mated for germ line transmission with Sv129 mice. One chimeric male transmitted the mutation from which the colony of mice has been obtained.

Reagents and probes. The antibodies anti-Akt1, anti-PTEN, anti-ILK, phospho-Akt (Thr308), and (Ser473) were obtained from Cell Signaling; anti-c-Jun and anti-PPARβ were from Affinity Bioreagents; anti-PDK1 was from Santa Cruz Biotechnology; antitubulin was from Pharmingen; anti-ADRP was from Progen; and anti-PL-I was from Chemicon.

The gene-specific probes for *PL-I* and *Tpbpa* were a kind gift of J. Rossant, and *Mash-2* was obtained from F. Guillemot. For preparing the probes, total RNAs were obtained from E9.5 placenta. cDNAs were prepared by reverse transcription, followed by PCR, using specific primers (primer sequences are available upon request). The cDNA corresponding to the mouse PPARβ and L27 were subcloned into pGEM3Zf(+) (Promega). The cDNA corresponding to the mouse PPARγ, as well as gene-specific probes corresponding to *PL-I*, *Id-2*, *Hand1*, *I-mfa*, *ADRP*, and *aP2*, was subcloned into pGEM-T Easy (Promega). Gene-specific antisense and sense riboprobes were synthesized by in vitro transcription with either T7 or Sp6 RNA polymerase (Ambion).

RPA. For all riboprobes, except L27, a ratio of 1:1 of [α-^{32}P]UTP to cold UTP was used, whereas a ratio 1:20 was used for L27 probe. An RNase protection assay (RPA) was carried out as described by the manufacturer (Ambion) with the following modifications. Briefly, total RNA was isolated from cells or tissues with Trizol reagent (Sigma, St. Louis, MO). Ten micrograms of total RNA was incubated at 37°C with 1 ng of gene-specific riboprobes (10^9 cpm/μg) and 10 ng of the L27 probe (10^7 cpm/μg). RNase digestion (10 U/ml RNase A; 400 U/ml RNase T_1) was carried out for all probes at 37°C for 20 min. After inactivation of RNase with 20 μl of 10% sodium dodecyl sulfate (SDS) and 10 μl of 20 mg/ml proteinase K for 20 min at 37°C, protected RNA was precipitated with 500 μl isopropanol, and RPA products were resolved in a 6% electrolyte-gradient denaturing polyacrylamide gel. Gels were then dried and exposed to X-ray film or to the phosphor screen of a StormImager 840 (Molecular Dynamics). Control RPAs were performed using an L27 antisense probe, which has been described previously (39). Quantitative analysis was performed by using IQuant 2.5 software.

In situ hybridization. Embryos and placentas were obtained by dissecting pregnant females, with the appearance of a vaginal plug being counted as day 0.5 of pregnancy. Because of their close contact, particularly at E9.5 stage, both the maternal decidua and the fetal part of the placenta were dissected as a whole. Embryos and placentas were separately fixed overnight at 4°C in 4% paraformaldehyde in phosphate-buffered saline (PBS) and embedded in paraffin, and 7-μm sections were cut. In situ hybridization was processed as described previously (5). Briefly, antisense and sense riboprobes for *PPAR*β, *Mash-2*, *Tpbpa* (or *4311*), and *PL-I* were generated by in vitro transcription of the corresponding cDNA clones with SP6 or T7 RNA polymerase. Rehydrated sections were washed in 2× SSC (1× SSC is 0.15 M NaCl plus 0.015 M sodium citrate) for 5 min, and hybridization was performed overnight at 70°C with 1 μg/ml of a digoxigenin-labeled probe in the following hybridization buffer: 50% formamide, 10% dextran sulfate, 1× Denhardt's solution, 1 mg/ml yeast RNA, 200 mM NaCl, 1.1 mM Tris-base, 8.9 mM Tris-HCl, 5 mM Na_2HPO_4, and 1.25 mM EDTA. Three washes of 30 min were done in 50% formamide, 1× SSC, and 0.1% Tween 20 at 65°C, followed by two washes in MABT (100 mM maleic acid, 140 mM NaCl, 1% Tween 20, pH 7.5). Sections were then incubated for 90 min in a blocking buffer consisting of 20% goat serum–2% blocking reagent (Boehringer Mannheim) in MABT and then left overnight at room temperature in an alkaline phosphatase-conjugated antidigoxigenin antibody (Boehringer Mannheim) at a dilution of 1:2,000 in a blocking buffer. Washes were done in MABT, five times for 30 min each time. Sections were then washed for 5 min in NTMT (100 mM NaCl, 100 mM Tris, 50 mM $MgCl_2$, 1% Tween 20, pH 9.5), and a color reaction assay was performed in the dark in nitroblue tetrazolium and 5-bromo-4-chloro-3-indolyl phosphate (Roche) and 1 mM levamisole in NTMT.

TABLE 1. Lethal stages of PPARβ$^{-/-}$ embryos

Stage	n^a	No. of embryos or pups by genotype (%)			No. of resorbed embryos[b]
		+/+	+/−	−/−	
E 9.5	259	71 (30)	119 (50)	50 (20)	19
E 10.5	47	12 (32)	20 (54)	5 (14)	10
E 12.5	54	10 (20)	38 (78)	1 (2)	5
E 14.5	21	6 (29)	15 (71)	0	0
P 21[c]	1820	626 (34)	1,165 (64)	29 (1.6)	

[a] *n*, number of embryos or pups analyzed.
[b] Resorbed embryos were not genotyped and not counted for the evaluation of the percentages of the different genotypes.
[c] P, postnatal day.

Immunohistochemistry. Immunohistochemistry was carried out on sections using the avidin-biotin-peroxidase method (Vector Laboratories) on 7-μm sagittal placental paraffin sections. Endogenous peroxidases were quenched by exposing the sections to 3% H_2O_2 for 5 min, followed by a wash in PBS. Nonspecific binding sites were blocked using 10% normal serum in 0.1% Triton-PBS for 1 h. Immediately after, the sections were incubated with the primary antibody for 1 h. After being washed in PBS, the slides were incubated with appropriate biotinylated secondary antibodies (1:200; Vector Laboratories) for 45 min, followed by 30 min in an avidin-biotin complex solution (Vector Laboratories) in PBS. The sections were then stained with 3,3′ diaminobenzidine (Sigma), rinsed in water, and counterstained with a 0.1% methyl-green aqueous solution for 5 min.

Western blots. For the Western blot of Fig. 1, nuclear extracts were obtained from the skin of mouse pups. Briefly, tissues were homogenized in 10 mM KCl, 1.5 mM $MgCl_2$ 10 mM HEPES, pH 7.9, 1 mM dithiothreitol, 1 mM Na_3VO_4, 10 μg/ml leupeptin, 0.3 trypsin inhibitor units (TIU)/ml aprotinin, 1 μM pepstatin A, and 1 mM phenylmethylsulfonyl fluoride. The homogenate was centrifuged at 2,000 × *g* for 10 min, and the pellet was washed with the same buffer. The washed pellet was resuspended in a buffer containing 420 mM NaCl, 10 mM KCl, 20 mM HEPES, pH 7.9, 20% glycerol, 1 mM dithiothreitol, 1 mM Na_3VO_4, and the protease inhibitors specified above.

For other experiments, Western blotting was performed on cells or tissues, lysed in an ice-cold lysis buffer (20 mM $Na_2H_2PO_4$, 250 mM NaCl, 1% Triton 100, 0.1% SDS) supplemented with complete protease inhibitors (Roche). After Bradford quantification (Bio-Rad), 10 μg of nuclear extracts or 30 μg of total protein was separated by SDS-polyacrylamide gel electrophoresis and transferred onto polyvinylidene difluoride membranes for Western blotting. The membranes were processed in the following steps: (i) 1 h of saturation in Tris-buffered saline (TBS)–0.1% Tween–5% nonfat milk at room temperature (RT), (ii) overnight incubation with a primary antibody in TBS–0.1% Tween–5% nonfat milk at 4°C, (iii) three washings in TBS–0.1% Tween at RT, (iv) exposure for 1 h to a secondary antibody in TBS–0.1% Tween–5% nonfat milk at RT, and (v) three washings in TBS–0.1% Tween at RT as a final step. The signal was detected using an ECL detection kit (Amersham Pharmacia Biotech), according to the manufacturer's instructions. Equal loading and transfer were verified by Coomassie blue staining of the membrane.

Rcho-1 trophoblast cell culture. Rcho-1 trophoblast cells were a kind gift from M. Soares. They were routinely maintained in a subconfluent condition with an RPMI 1640 culture medium supplemented with 10% fetal bovine serum (FBS), 50 μM β-mercaptoethanol, 1 mM sodium pyruvate, 2 mM glutamine, 100 U/ml of penicillin, and 100 μg/ml of streptomycin in a humidified incubator under 5% CO_2–95% air at 37°C. Differentiation was induced by growing the cells to confluence and subsequently replacing the 10% FBS supplementation with 1% horse serum. The change to differentiation medium is indicated as day 0.

Design and cloning of lentiviral siRNA vectors. (i) Vector construction. The target sequence (19 nucleotides) was chosen in the mouse *PPAR*β sequence 5′-GCACATCTACAACGCCTAC-3′. This sequence has identity in 18 of 19 residues with the rat *PPAR*β sequence (the underlined residue in rat *PPAR*β is a T) and was also efficient in the Rcho-1 cells of rat origin. A BLAST search ensured that the sequences would not target other RNAs, including PPARγ mRNAs, in a nonspecific manner. The short interfering RNA (siRNA) was cloned in a lentivirus vector in which the mouse *PPAR*β siRNA was under the control of the polymerase III-dependent H1 promoter. In addition, an internal cassette allowed the expression of the green fluorescent protein (GFP) marker

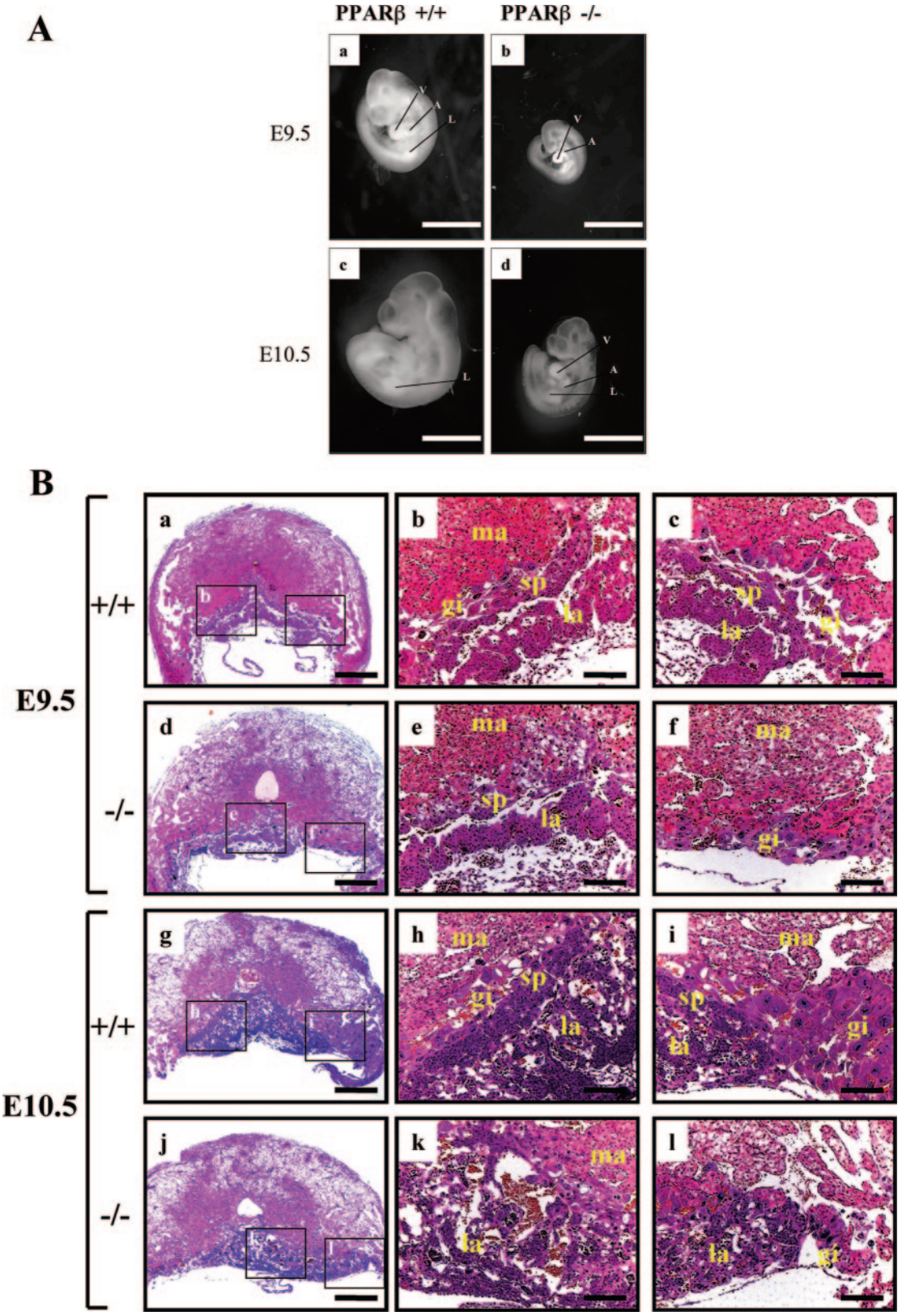

FIG. 2. Defects in extra-embryonic tissues associated with the PPARβ-null genotype. (A) Morphology of E9.5 and E10.5 embryos from wt (a and c) and PPARβ$^{-/-}$ (b and d). (B) Hematoxylin-eosin-stained sections of wt (a to c and g to i) and PPARβ-null (d to f and j to l) placentas. Higher magnification views of PPARβ-null placenta at E9.5 (e and f) and E10.5 (k and l) show a severe reduction of the giant cell layer in the mutant. A, heart atrium; gi, trophoblast giant cells; L, limb; la, labyrinthine trophoblast; ma, maternal decidual tissue; V, heart ventricle; sp, spongiotrophoblast. Bars = 1 mm (A), 400 μm (B, frames a, d, g, and j), and 100 μm (B, frames b, c, e, f, h, i, k, and l).

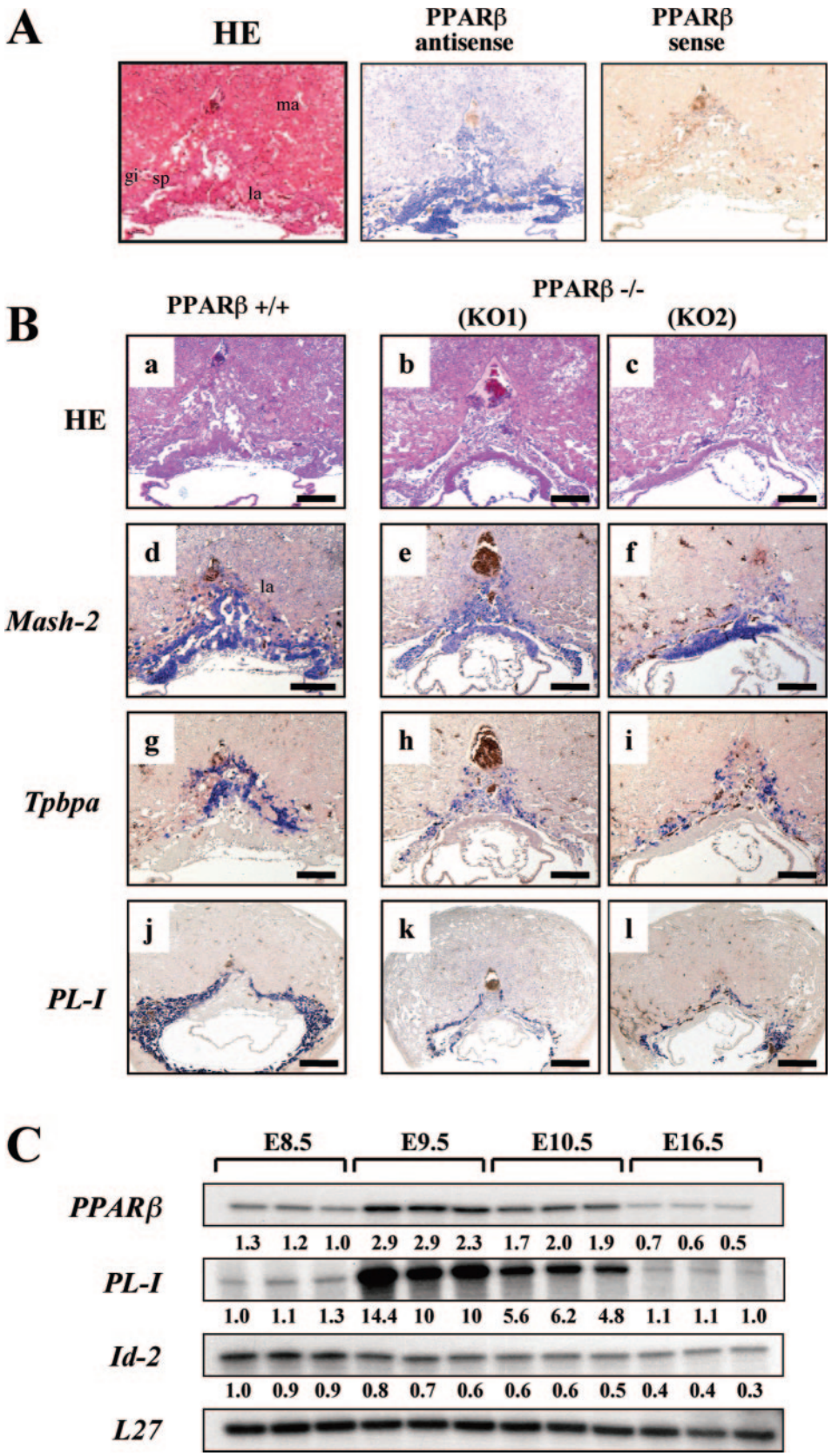

FIG. 3. Expression of trophoblast markers in wt and in PPARβ mutant placentas. (A) Spatial expression of PPARβ mRNA in E9.5 wt placenta. Left, hematoxylin-eosin (HE) staining; middle, in situ hybridization with digoxigenin-labeled antisense riboprobe for PPARβ; right, control with sense riboprobe. Scale bar, 200 μm. (B) Representative E9.5 placenta sections from one wt (a, d, g, and j), and two PPARβ mutant KO1 (b, e,

gene under the control of the EF-1α promoter. A full description of the vector is given in by Wiznerowicz and Trono (65). In our study, the control vector, which contains all the features but not the siRNA, was called LV-TH and the siRNA-containing vector was named LV-THsiPPARβ.

(ii) Lentivirus production. All recombinant lentiviruses were produced by transient transfection of 293T cells according to standard protocols. Briefly, subconfluent 293T cells were cotransfected with 20 μg of the control vector pLV-TH or the PPARβ-targeted vector pLV-THsiPPARβ, 15 μg of pCMV-ΔR8.91, and 5 μg of pMD2G-VSVG (where CMV is cytomegalovirus and VSVG is vesicular stomatitis virus protein G) by calcium phosphate precipitation. The medium was changed after 16 h, and recombinant lentiviruses were harvested 24 h later.

(iii) Controlling lentivirus infection and silencing efficiency. The efficiency of the transduction was given by the percentage of GFP-expressing cells. At a multiplicity of infection of 60, 90% of the Rcho-1 cells expressed GFP. The efficiency of the siRNA on rat *PPAR*β sequence was measured by transducing Rcho-1 cells with LV-THsiPPARβ or the control LV-TH vector at a multiplicity of infection of 60. Forty-eight hours later, the cells were harvested, and total RNA was extracted. The level of expression of PPARβ was measured by RPA.

Oil red O staining. Cultured Rcho-1 cells or sagittal sections of mouse placenta were washed in PBS and fixed in 4% paraformaldehyde for 10 min at 4°C. A fresh working solution of oil red O (Sigma Chemical, St. Louis, MO) was prepared by dilution of the oil red O stock solution (5 g/liter in 98% isopropanol) in distilled water at a ratio of 3:2. The working solution was allowed to stand for 10 min after mixing and was filtered with a 0.45-μm-pore-size filter. Subsequently, sections were stained in oil red O for 10 min, washed in tap water, and counterstained with a 0.1% methyl-green aqueous solution for 5 min. The slides were allowed to dry and were mounted with Vectashield mounting medium (Vector Laboratories, Burlingame, CA).

RESULTS

Growth and lethality of PPARβ$^{-/-}$ embryos. To assess the physiological role of PPARβ in the whole organism, particularly during development, the *PPAR*β gene was disrupted in ES cells by homologous recombination, following the strategy described in Materials and Methods and in the legend of Fig. 1. The PPARβ$^{+/-}$ mice (of mixed background C57BL6/Sv129) were healthy, fertile, and displayed no obvious aberrant phenotype. However, heterozygote mating did not produce the expected Mendelian ratio of mutant animals (Table 1), as the PPARβ$^{-/-}$ live animals were very rare (~1.6% instead of the expected 25%) while no perinatal death was observed. The sacrifice of gestating mice from heterozygote mating revealed segregation ratios that were close to normal at E9.5 for the disrupted *PPAR*β alleles among embryos. Beyond this stage, the number of live PPARβ$^{-/-}$ embryos decreased, and by E14.5, no living PPARβ$^{-/-}$ embryos were detected in the litters sacrificed, indicating that the homozygous disruption of PPARβ resulted in a highly penetrant embryonic lethality. The E9.5 live PPARβ$^{-/-}$ mutant embryos presented various degrees of developmental retardation, with severe growth retardation but in most cases no gross abnormalities (Fig. 2A). Significantly, the placenta of PPARβ$^{-/-}$ concepti appeared small and abnormal, as previously observed by Barak et al. (2).

Surprisingly, around 1% of the expected number of homozygotes lived through birth. These rare PPARβ-null progeny exhibited growth retardation, which was overcome by the time the animals reached adulthood. Because the rarity of live homozygous pups obtained from heterozygote mating precluded the possibility of constituting experimental groups of sufficient size, we intercrossed PPARβ$^{-/-}$ mice. Both male and female mutants were subfertile, and the number of nonproductive breeding pairs was elevated in the PPARβ-null mice. However, a PPARβ$^{-/-}$ mouse colony was established after selection of a few successful breeding pairs, for which the total number of pups born per productive breeding pair as well as the mean litter size was significantly lower (4 ± 2 pups) compared to control heterozygous matings (7 ± 2 pups). In parallel, we designed a new distinct homologous recombination strategy and generated a second, totally independent, PPARβ mutant mouse line. This second mutant line, which carries a deletion of the exon 4 disrupting the open reading frame of the corresponding mRNA, displayed exactly the same phenotype (early embryonic lethality of high but not full penetrance) as the one used in the present study (data not shown).

This reproducible phenotype pointed to a major role of PPARβ in regulating some cellular and tissular processes taking place during placental development and was thus subjected to an in-depth analysis.

Defining the placenta alterations in PPARβ$^{-/-}$ concepti. For histological inspection, only placentas obtained from fetuses that were not dead in utero, as judged by a beating heart and absence of necrosis signs, were analyzed in order to exclude artifacts from postmortem placental alterations. At E9.5, the placentas of PPARβ$^{-/-}$ embryos, compared to those of PPARβ$^{+/+}$ littermate embryos, were reduced in size and very compact (Fig. 2B). The three main placenta layers, i.e., the trophoblast giant cells, the spongiotrophoblast, and the labyrinthine layers were altered. Similar defects were observed at E10.5, showing that the defect was not merely a delay in placental development (Fig. 2B). We also sacrificed homozygous females mated with homozygous males at day 9.5 post coitum. At that stage, the litter size was close to normal (between 7 and 10 embryos), but many concepti exhibited similar placental defects as those seen in PPARβ$^{-/-}$ concepti from heterozygous mating (see supplemental information at http://www.unil.ch/webdav/site/cig/shared/desvergne/Nadra_et_al_supp_data.pdf). The normal litter size at E9.5, but reduced litter size at birth, indicated that lethality also occurred in homozygous matings, as expected from histological studies of the placenta. These observations established that the defect was also present in homozygous breeding, but the penetrance was somehow milder, allowing the birth of approximately 30% of the PPARβ$^{-/-}$ pups. Thus, these histological observations indicated that in PPARβ$^{-/-}$ placentas, the overall structure of the placenta is affected. Further analyses were therefore required in order to define the primary defect.

h, and k) and KO2 (c, f, i, and l) littermates. HE corresponds to standard staining with hematoxylin-eosin. Mash-2 is a marker for spongiotrophoblast and labyrinthine trophoblast cells; Tpbpa is a specific marker of spongiotrophoblast cells; PL-I specifically labels trophoblast giant cells. Scale bars, 200 μm (a to i) and 400 μm (j to l). (C) Relative mRNA expression of PPARβ, PL-I, and Id-2 in mouse placental tissues from E8.5, E9.5, E10.5, and E16.5. L27 ribosomal protein mRNA was used for normalization. Three independent samples are shown per condition. Numbers represent the relative increase (*n*-fold) with respect to the basal level evaluated at E8.5 time points. gi, trophoblast giant cells; la, labyrinthine trophoblast; ma, maternal decidual tissue; sp, spongiotrophoblast.

We first analyzed whether there was a spatial specificity of PPARβ expression in the E9.5 developing placentas. However, in situ hybridization in wt placentas showed that PPARβ mRNA is ubiquitously expressed throughout the placenta including the labyrinth, the spongiotrophoblast, and the giant cells (Fig. 3A). We thus evaluated the different trophoblast layers in the mutant placentas using a series of specific markers. The bHLH transcription factor Mash-2 is mainly expressed in the trophoblast cells of the spongiotrophoblast and labyrinth layer (23). In situ hybridization performed with a murine Mash-2 probe showed that the labyrinthine layer expressing Mash-2 was thinner in PPARβ mutants (Fig. 3B). In parallel, the spongiotrophoblast cell layer, characterized by the expression of the trophoblast-specific protein Tpbpa (also called 4311) (40), was also reduced in PPARβ mutant placentas, consistent with the histological analysis described above (Fig. 3B) (see also supplemental information at http://www.unil.ch/webdav/site/cig/shared/desvergne/Nadra_et_al_supp_data.pdf). The expression profile of PL-I is especially useful in characterizing early molecular events underlying trophoblast differentiation, since transcription of this gene occurs exclusively in giant cells and begins at the time of implantation (40, 47). Interestingly, we consistently observed in PPARβ mutant placenta the most severe reduction in the thickness of the PL-I-expressing layer (Fig. 3B). Thus, while all layers were affected, the marker analyses underscore the severe alteration of the giant cell layer.

To examine the possibility of a relationship between PPARβ and trophoblast giant cell differentiation, we performed a quantitative analysis of the temporal expression of PPARβ, PL-I, and Id-2 in wt placentas by RPA. Id-2 is an inhibitor of bHLH transcription factors. It is highly expressed in trophoblast progenitor cell populations and is down-regulated upon induction of giant cell differentiation (8) (48). RPA analysis performed at E8.5, E9.5, E10.5, and E16.5 showed a parallel expression between PPARβ and PL-I, with a similar peak of expression at E9.5 followed by a decrease at E10.5. Consistently, Id-2 expression was maximal at E8.5 and decreased at E9.5, remaining low but detectable (Fig. 3C). Thus, the combination of the spatiotemporal expression pattern of PPARβ with that of several placenta markers indicates that PPARβ may act directly to regulate trophoblast giant cell differentiation.

PPARβ is required for trophoblastic giant cell differentiation. The putative direct role of PPARβ in affecting giant cell differentiation was explored in the Rcho-1 trophoblast cell line, which provides a reliable system for the molecular analysis of the giant cell differentiation process (15, 25). When cultured in a regular 10% FBS-containing medium, these cells remain in proliferation and can be regularly subcultured while maintaining an undifferentiated status. The change from 10% FBS to 1% horse serum causes the cells to cease their proliferation and corresponds to the initiation of their differentiation into trophoblast giant cells (time zero). To evaluate the role, if any, of PPARβ in this process, we exposed the cells from time zero to the PPARβ agonist L-165041 and used cell morphology and PL-I expression as readouts of the differentiation status. At day 4 of the experiment, only a few control cells exhibited the features of differentiated cells; this was expected since the full differentiation process usually requires 6 to 8 days (25). Strikingly, the addition into the medium from day 0 onwards of the specific PPARβ agonist L-165041 triggered a massive early differentiation (Fig. 4A) accompanied by a major increase of PL-I mRNA levels and severe reduction of Id-2 mRNA (Fig. 4B). Western blot analyses confirmed the very high levels of PL-I expressed in these cells (Fig. 4C). Because Rcho-1 cells expressed both PPARβ and PPARγ (Fig. 5A, top lines), the specific PPARγ ligand rosiglitazone (RSG) was also tested but was found to have no effect on PL-I expression and giant cell differentiation (Fig. 4C).

To demonstrate that PPARβ is indeed required for trophoblast giant cell differentiation, we silenced PPARβ gene expression in the Rcho-1 cells and then assessed their ability to differentiate. Silencing was obtained via infection with a lentivirus expressing a PPARβ siRNA (LV-THsiPPARβ), as described in Materials and Methods. Cells infected with a control lentivirus (LV-TH; see Materials and Methods) or noninfected cells were used as controls. RPA analyses showed that cells transduced with LV-THsiPPARβ had around 70% less PPARβ mRNA than the LV-TH control vector-infected cells and noninfected cells, which displayed similarly high levels of PPARβ mRNA (Fig. 4D). As expected, the control cells reacted to the PPARβ agonist by a massive differentiation. In contrast, and at the same time point, only a few cells were undergoing differentiation when infected with the siRNA-containing lentivirus (Fig. 4E, right panels). RPA analyses also confirmed the low level of PL-I expressed in these cells after 4 days of exposure to the PPARβ ligand (Fig. 5C). This clearly demonstrates that PPARβ is required for the L165041-mediated accelerated differentiation of Rcho-1 cells into trophoblastic giant cells. More importantly, we also analyzed the behavior of Rcho-1 cells under the regular differentiation protocol, which we prolonged up to 15 days. Fifteen days after the initiation of differentiation by serum replacement, noninfected and control LV-TH-transduced cells exhibited the expected features of differentiated cells, as evaluated by the increased nuclear size. In contrast, the LV-THsiPPARβ-infected cells remained undifferentiated (Fig. 4F). These results clearly demonstrate the strict requirement of PPARβ expression for giant cell differentiation.

PPARβ acts on giant cell differentiation via the PI3K/Akt signaling pathway and I-mfa expression. Among the factors known to contribute to giant cell differentiation, Hand1 is a bHLH transcription factor that promotes giant cell differentiation in early postimplantation mouse embryos (53, 56). In contrast, Mash-2, which is mainly expressed in the spongiotrophoblast and labyrinthine layers, as mentioned above, must be inhibited for the differentiation to occur. This is in part performed by I-mfa, a non-HLH inhibitor of the myogenic bHLH subfamily, which inhibits the transcriptional activity of Mash-2 by preventing its nuclear localization (7, 36). Id-2 acts as a negative regulator of bHLH transcription factors, and its down-regulation is required for trophoblast development (8). According to these elements, we first hypothesized that PPARβ might promote giant cell differentiation via induction of Hand1 activity. However, the expression of Hand1 did not change upon PPARβ-mediated induction of Rcho-1 differentiation into giant cells (Fig. 5A). In contrast, the alternative mechanism, via inhibition of Mash-2 activity, is supported by the diminished expression of Id-2 and an increased expression of I-mfa that parallels PL-I induction (Fig. 5A).

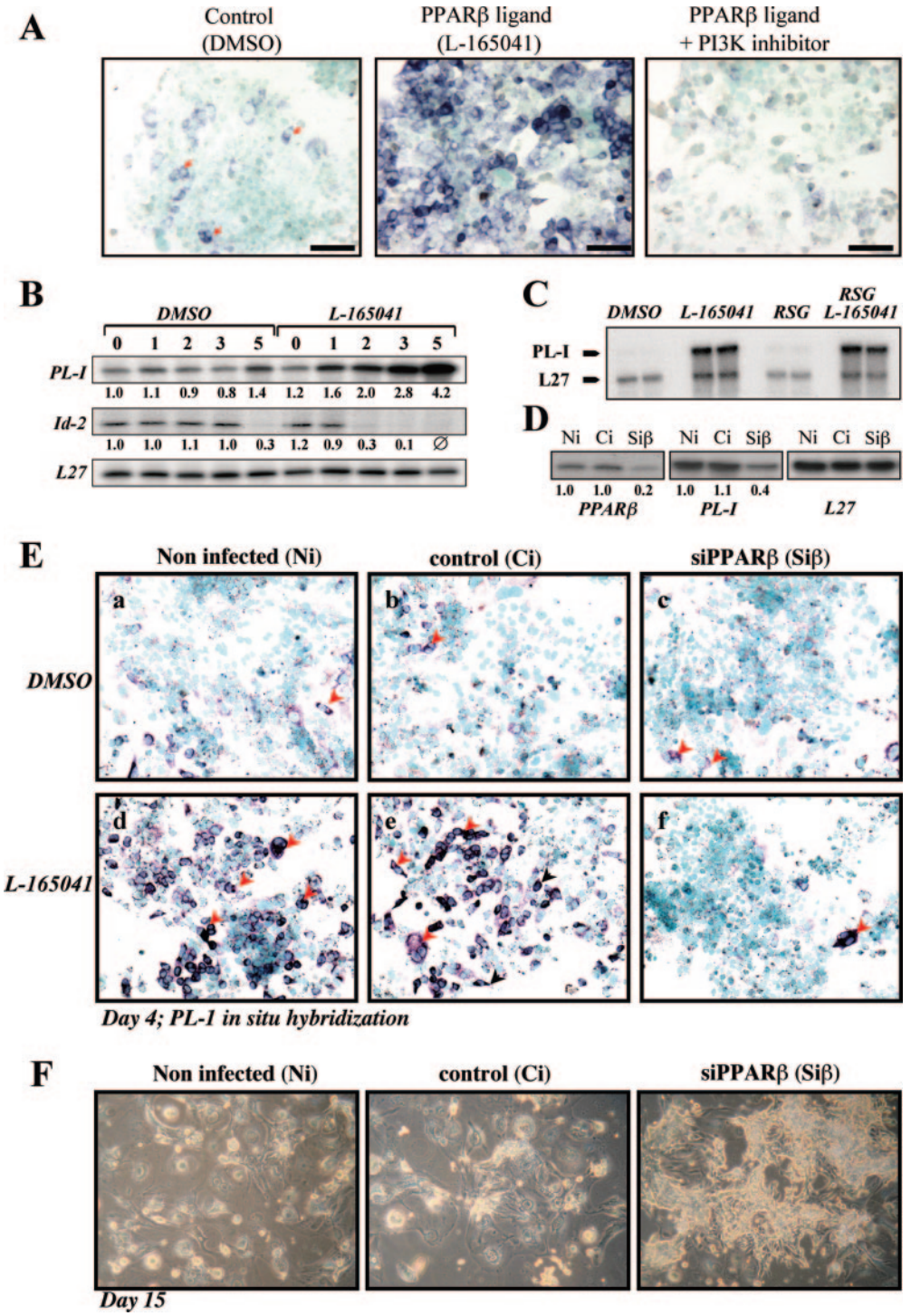

FIG. 4. PPARβ-dependent differentiation of Rcho-1 cells in trophoblast giant cells. Rcho-1 cells were grown to 60% confluence. The change to 1% horse serum-containing medium defines the time zero of the differentiation process. (A) Expression of PL-I in Rcho-1 cells after 4 days of differentiation in the presence of dimethyl sulfoxide (DMSO) (0.05%) used as a vehicle, the PPARβ agonist L-165041 (5 μM), the PPARβ agonist and the PI3K inhibitor LY294002 (10 μM). Scale bar, 80 μm. (B) Temporal expression of PL-I and Id-2 in differentiating Rcho-1 cells cultured in the presence of L-165041 or of its vehicle dimethyl sulfoxide (DMSO), as indicated. Numbers represent relative increase (*n*-fold) with respect to basal level in the presence of dimethyl sulfoxide (0.05%) at time zero. (C) Effect of RSG (1 μM) on PL-I expression after 4 days of treatment. Two independent duplicates per condition are shown. (D) Silencing of PPARβ in Rcho-1 cells. The Rcho-1 cells were noninfected or transduced with a control lentivirus vector (LV-TH), or with a vector producing a PPARβ-specific siRNA (LV-THsiPPARβ). Silencing efficiency was established by measuring the mRNA levels of PPARβ after 15 days of the differentiation protocol. L27 ribosomal protein mRNA was used as an internal control. (E) Differentiation of Rcho-1 cells either noninfected, transduced with LV-TH, or transduced with LV-THsiPPARβ. In situ hybridization with PL-I probe was used as a marker of giant cell differentiation at day 4 of differentiation in the presence of L-165041 (5 μM) or its vehicle (dimethyl sulfoxide). Red arrowheads show some of the differentiated cells that express PL-I. The nuclei were stained with a methyl-green solution. (F) Bright-field images of Rcho-1 cells in culture after 15 days of differentiation. Ni, noninfected; Ci, LV-TH; Siβ, LV-THsiPPARβ/δ.

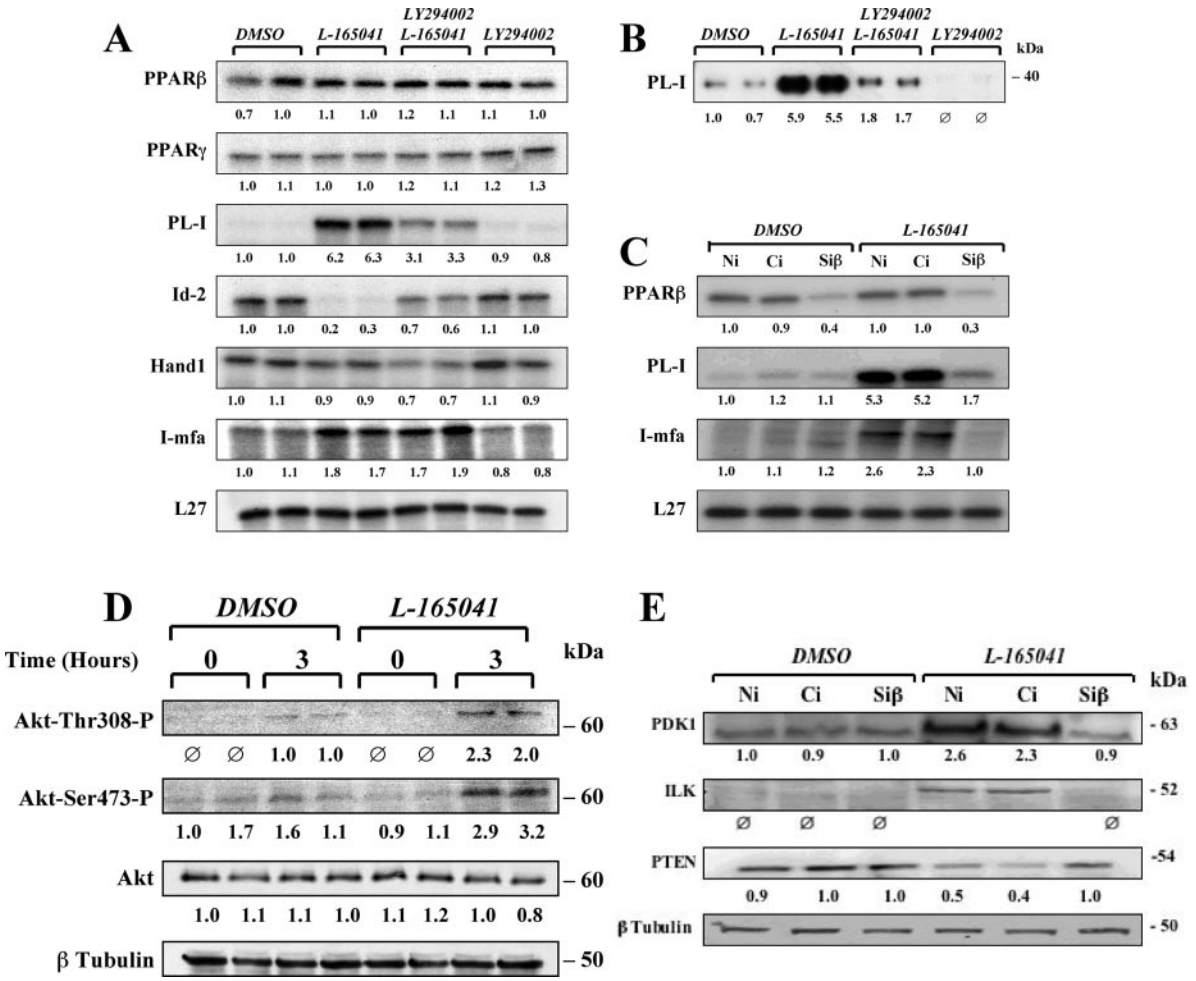

FIG. 5. PPARβ promoting giant cell differentiation requires an intact PI3K/Akt pathway. (A) mRNA expression levels of PPARβ, PPARγ, PL-I, Id-2, Hand1 and I-mfa after 4 days of indicated treatments with L-165041 (5 μM) and/or PI3K inhibitor (LY294002) (10 μM). Two independent duplicates per condition are shown. (B) Western blot analysis of PL-I production in Rcho-1 cells treated by PPARβ ligand and/or by LY294002. Two independent duplicates per condition are shown. The number of cells seeded in each plate was accurately quantified at the beginning of the experiment, and all culture conditions were strictly comparable. (C) mRNA expression levels of PPARβ, PL-I, and I-mfa in Rcho-1 cells either noninfected (Ni), transduced with the LV-TH (Ci), or transduced with the LV-THsiPPARβ (Siβ), after 4 days of differentiation in the presence of either dimethyl sulfoxide, used as a vehicle, or 5 μM PPARβ ligand. L27 ribosomal protein mRNA was used as an internal control. (D) Relative expression of phosphorylated Akt from Rcho-I trophoblast cells treated for 3 h with either vehicle or 5 μM PPARβ ligand. Total cellular proteins from Rcho-1 cells were used for Western blot analysis. Two independent duplicates per condition are shown. (E) Relative expression of PDK1, ILK, and PTEN in Rcho-1 cells either noninfected, transduced with the LV-TH, or transduced with the LV-THsiPPARβ, after 4 days of differentiation in the presence of either dimethyl sulfoxide, used as a vehicle, or 5 μM PPARβ ligand. Tubulin was used as an internal control. The apparent molecular mass is indicated for each protein. Numbers represent relative increase (*n*-fold) with respect to the basal level in the presence of dimethyl sulfoxide (0.05%) (A and B), to basal level to (Ni) in the presence of dimethyl sulfoxide (0.05%) (C and E) or to the level at time zero in the presence of dimethyl sulfoxide (0.05%) (D). DMSO, dimethyl sulfoxide; Ni, noninfected; Ci, LV-TH; Siβ, LV-THsiPPARβ.

Using the same Rcho-1 cellular model, Kamei et al. (33) have described the role of the PI3K signaling pathway in giant cell differentiation. To examine whether the PPARβ-mediated regulation of the different factors was dependent on the PI3K pathway, Rcho-1 cells were treated with the PPARβ ligand in the presence of LY294002, a specific PI3K inhibitor. Remarkably, the addition of LY294002 efficiently prevented the PPARβ-mediated up-regulation of PL-I mRNAs (Fig. 5A) and protein (Fig. 5B). This reduction of PPARβ activity was also observed with respect to Id-2 repression (Fig. 5A). In contrast, the PI3K inhibitor did not affect the PPARβ-induced expression of I-mfa. However, I-mfa expression remains PPARβ dependent since it was abolished in PPARβ siRNA-expressing cells (Fig. 5C). Further downstream of PI3K activation is the phosphorylation of Akt at the residues Ser473 and Thr308. Consistent with the results described above, treatment of Rcho-I cells with the PPARβ ligand for 3 h resulted in the phosphorylation of Akt1 (Fig. 5D).

These observations indicate that PPARβ activates Akt-1, which subsequently triggers the giant cell differentiation. We previously identified two kinases, namely, PDK1 and ILK, which in wounded skin regulate the PI3K/Akt pathway and which are direct PPARβ target genes (11, 12). As shown in Fig. 5E, both kinases were well expressed in control Rcho-1 cells

treated with the PPARβ agonist, whereas they were markedly reduced in LV-THsiPPARβ. We also measured the levels of phosphatase and tensin homolog deleted on chromosome 10 (PTEN), which negatively regulates the PI3K-mediated pathway by increasing the conversion from PiP3 to PiP2. Conversely, the loss of PTEN leads to Akt activation (21). PTEN levels were diminished in control Rcho-1 cells exposed to PPARβ agonist but remained similar to those of the nondifferentiated cells in PPARβ siRNA-treated cells (Fig. 5E).

These results demonstrate that PPARβ is essential for the full differentiation of trophoblast giant cells through the activation of the PI3/Akt1 signaling pathway, in addition to a PI3K-independent induction of I-mfa.

The pathways responsible for giant cell differentiation are altered in PPARβ mutant placenta. To demonstrate the relevance of the observations obtained in the Rcho-1 culture system, we biochemically characterized the trophoblastic giant cell layer by quantifying the expression levels of PL-I, Hand1, I-mfa, and Id-2 at E9.5 in control and PPARβ mutant placentas. Consistent with the results obtained in Rcho-1 cells, PL-I, Hand1, and I-mfa mRNA levels were markedly reduced in PPARβ mutant placenta compared with wt placenta. These decreased PL-I, Hand1, and I-mfa expressions were associated with a moderate increase in Id-2 mRNA levels (Fig. 6A).

We also analyzed the PI3K/Akt pathway in these placentas. The level of PDK1, as evaluated by Western blotting, was dramatically lower in the E9.5 PPARβ mutant placentas. Consistently, whereas the total amount of Akt1 protein was similar in wt and PPARβ mutant placentas, the phosphorylated forms of Akt at Ser473 and Thr308 were markedly reduced in the PPARβ mutant placentas compared to wt placentas (Fig. 6B). Recent studies have shown that Akt1 is expressed in all types of trophoblast cells and vessel endothelial cells in E14.5 wt placenta (67), but little is known about Akt activity at earlier stages. To further explore in vivo the relationship between Akt activity and trophoblast giant cells, we performed immunohistochemical staining with an antibody specifically recognizing Thr308-phospho-Akt1 (Akt-Thr308-P) and studied its localization in E9.5 wt placentas. Interestingly, Akt-Thr308-P was strongly detected in the trophoblast giant cells, where it was specifically located in the cell nucleus (Fig. 6C).

Together, these results demonstrate that the major role played by PPARβ in giant cell trophoblast differentiation through activation of the PI3K/Akt1 pathway, which we characterized in cell culture, also occurs in vivo.

PPARβ, lipid metabolism, and ADRP expression in giant cells. Placental fatty acid transfer is critical for normal fetal development, particularly for membrane biosynthesis, energy needs and storage, and synthesis of precursors of signaling molecules. In that respect, the labyrinth zone exerts a crucial role in regulating the bidirectional exchange between maternal and fetal compartments, with a facilitated directional flux of fatty acids from the mother to the fetus (28). Insufficient fatty acid supply may indeed result in retarded fetal growth (9). Little is yet known about the molecular mechanism of fatty acid transfer, while even less is known about fatty acid metabolism in the placenta in the early stages, when the labyrinth is not yet fully developed. The severe growth retardation observed in the PPARβ mutant embryos at E9.5 (Fig. 2) and the role of PPARβ in lipid metabolism (3, 17) led us to investigate

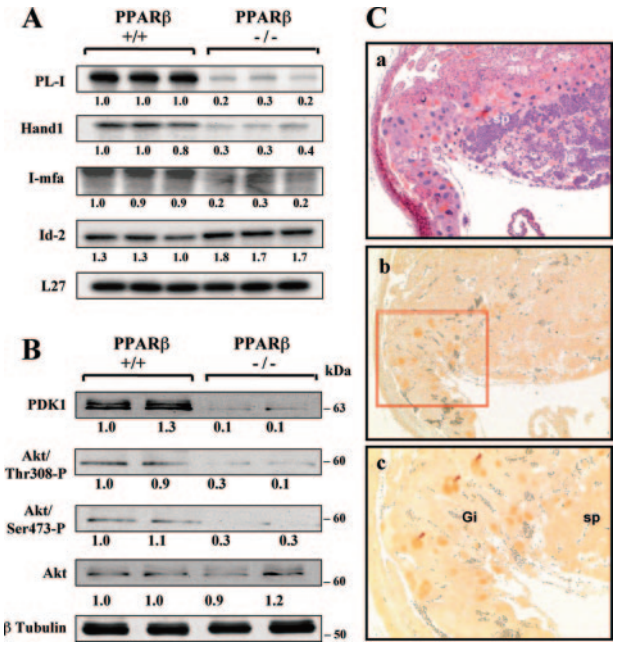

FIG. 6. Reduced Akt activity in PPARβ$^{-/-}$ embryos. (A) Expression profiles of PL-I, Hand1, I-mfa, and Id-2 at E9.5 in PPAR wt and mutants. L27 ribosomal protein mRNA was used as an internal control. Three independent samples are shown per genotype. (B) Relative expression of PDK1, Akt phosphorylated in Thr308 or in Ser473, and total Akt in PPARβ wt and mutant placenta at E9.5. Tubulin was used as an internal control. Total cellular proteins from E9.5 placentas were used for these Western blot analyses. The apparent molecular mass is indicated for each protein. Two independent samples are shown per genotype. (C) wt E9.5 placenta. Hematoxylin-eosin staining is shown in frame a. Immunohistochemistry (b and c) reveals the Thr308-phosphorylated Akt (Akt-Thr308-P) in the nuclei of giant cells (red arrowheads). The red square in frame b indicates the region seen in frame c at higher magnification. Numbers in panels A and B represent the relative increase (*n*-fold) with respect to basal level to wt.

the lipid status in E9.5 placentas, in comparison with the situation observed at E16.5.

As a first step, we assessed the presence and location of lipid droplets in the placenta, by oil red O staining of tissue sections of placentas. Strikingly, lipid accumulation was already observed at E9.5, remarkably pronounced in the giant cells (Fig. 7A, frames a to d) and to a lesser extent in the labyrinth part. At E16.5, the giant cells were no longer distinguishable, and lipid droplets were abundantly found in both the maternal decidua and the labyrinth, while they were undetectable in the spongiotrophoblast (Fig. 7A, frames e to h). This lipid accumulation in the form of cytosolic droplets was paralleled by the expression pattern of ADRP, a major lipid droplet-associated protein that helps in packaging neutral lipids into discrete lipid storage droplets in the cytoplasm (31). At E9.5, ADRP immunoreactivity was mainly localized in the cytoplasm of trophoblast giant cells (Fig. 7B, frames a to d). Higher magnification revealed the particular pattern of ADRP protein localized as brown rings around the lipid droplets (Fig. 7B, frame d). In the labyrinthine trophoblast cells, ADRP was found toward the apical surface of the cells and was concentrated along the fetal vessels (Fig. 7B). At E16.5, ADRP was abundantly expressed

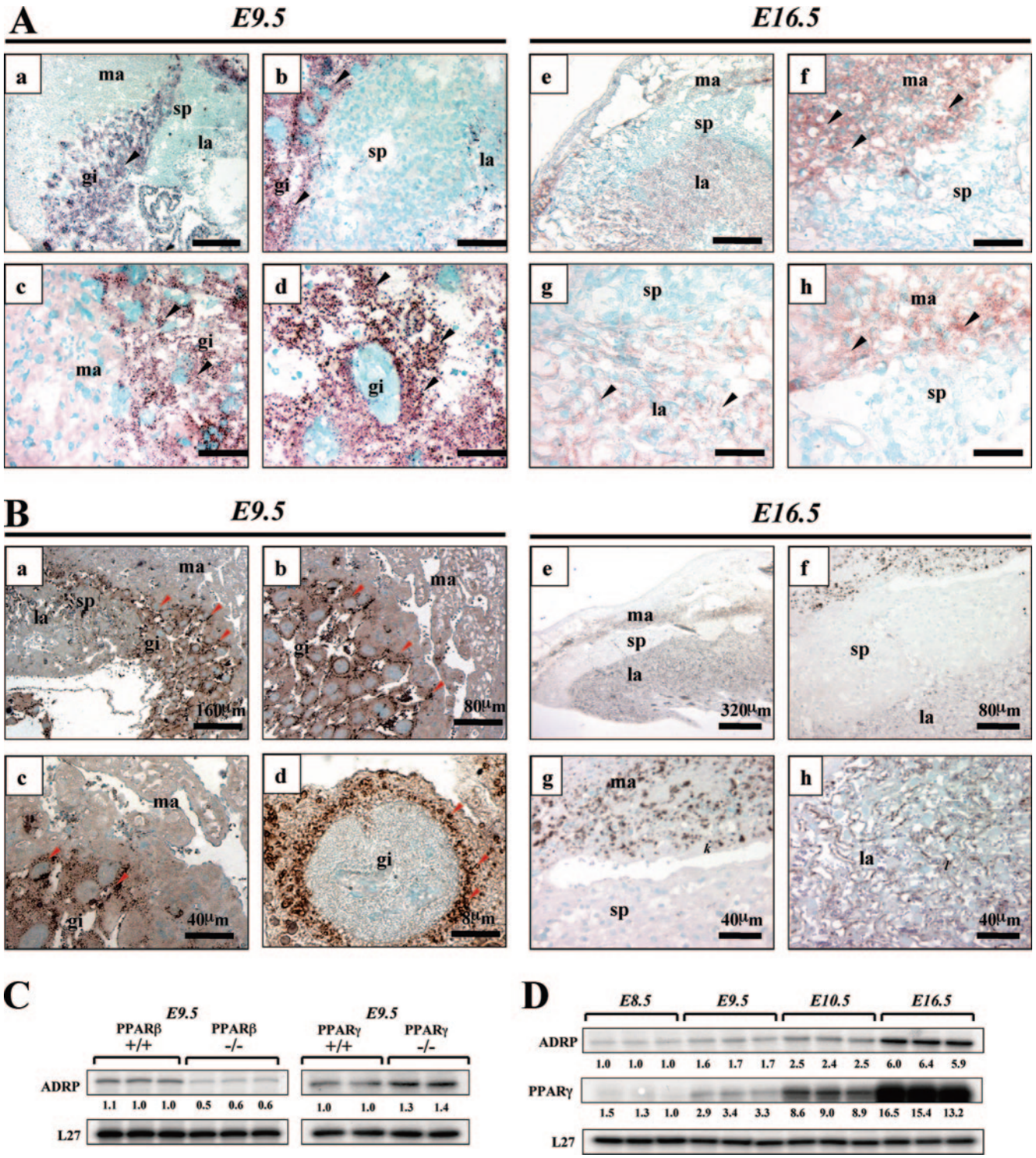

FIG. 7. Lipid storage droplets accumulate in the mouse placenta. (A) Oil red O staining of sagittal sections of mouse placenta at E9.5 (a to d) and E16.5 (e to h). Abundant small lipid droplets were observed inside the cytoplasm of trophoblast giant cells. As seen in frame d, the droplets are particularly localized near the nucleus. Black arrowheads indicate some lipid droplets. Bars: 200 μm (a and e), 40 μm (b, c, and f), 20 μm (g and h), and 8 μm (d). (B) Distribution of ADRP in mouse placenta at E9.5 (a to d) and E16.5 (g to j). Red arrowheads indicate some specific labeling corresponding to ADRP protein. (C) Expression profile of ADRP mRNA in E9.5 placentas from PPARβ wt and mutant concepti (left) and from PPARγ wt and mutant concepti (right). (D) Relative mRNA expression profiles of ADRP and PPARγ in mouse placental tissues from E8.5, E9.5, E10.5, and E16.5. L27 ribosomal protein mRNA was used for normalization. Numbers represent the relative increase (*n*-fold) with respect to the basal level at E8.5 (D) or to wt (C). gi, trophoblast giant cells; la, labyrinthine trophoblast; ma, maternal decidual tissue; sp, spongiotrophoblast.

in the decidua and the labyrinth (Fig. 7B, frames e to h), closely reproducing the lipid droplet pattern.

A quantitative evaluation of ADRP expression by RPA showed that ADRP mRNA levels were very low at E8.5 and continuously increased with time, reaching high levels at E16.5 (Fig. 7D). We then explored the respective roles of PPARβ and PPARγ in regulating ADRP expression. For that purpose, we took advantage of the targeted disruption of the *PPAR*γ allele, described by Rieusset et al. (52), to compare ADRP expression in PPARβ null and PPARγ null mutant placentas at E9.5. Strikingly, ADRP mRNA levels were markedly reduced in PPARβ mutant placentas (Fig. 7C), consistent with the strong alteration of the giant cell layer. In contrast, PPARγ mutant placentas exhibited minimal changes, with a tendency to an increase in ADRP mRNA levels (Fig. 7C), clearly demonstrating that at this stage of placental development, ADRP is mainly expressed in the giant cells and under the direct or indirect control of PPARβ but not of PPARγ. No mutant placentas could be obtained at E16.5, but at this stage, there is a remarkable parallel in wt placentas between the intense labyrinth ADRP immunostaining, the high levels of ADRP mRNA, and the high levels of PPARγ mRNA (Fig. 7D). This suggests that the expression of ADRP in the labyrinth at later stages of placental development is under the control of PPARγ. Whereas this is consistent with a previous report showing a PPARγ-dependent increase in ADRP expression in human trophoblast cells (4), the control of ADRP expression at the late placental stage remains to be analyzed.

ADRP expression is associated to giant cell differentiation and under the control of PPARβ. To evaluate whether ADRP expression and lipid droplet accumulation in the giant cells were due to the placental environment or could be precisely attributed to giant cell functions, we furthered our investigations in Rcho-1 cells. Amazingly, an increase in ADRP expression and the appearance of lipid droplets accompanied giant cell differentiation, obtained either using the classical procedure or by accelerated differentiation via exposure to a PPARβ ligand. In this context, PPARγ ligand RSG provoked little if any increased ADRP expression. The need for PPARβ was further shown in cells infected by LV-THsiPPARβ, which prevented the PPARβ ligand-induced expression of ADRP (Fig. 8A).

While a peroxisome response element (PPRE) has been identified in the ADRP mouse promoter, suggesting a direct transcriptional regulation of ADRP (6), the mechanism by which PPARβ increased ADRP expression during trophoblast giant cell differentiation also relies on PPARβ-dependent PI3K activity. Indeed, in cells treated with the PI3K inhibitor, the expression of ADRP dropped to the same extent as the other giant cell markers (Fig. 8A). This emphasizes the fact that control of ADRP expression cannot be dissociated from the overall process of giant cell differentiation regulated by PPARβ. To assess whether ADRP is truly under the control of PPARβ, we evaluated its expression in adult tissues from mutant mice. In the white adipose tissue of PPARβ mutant mice, ADRP expression decreased by twofold, whereas the adipocyte fatty acid binding protein (aFABP/aP2), used as an adipocyte marker, only decreased slightly (Fig. 8B). In contrast, the mRNA levels of ADRP and aP2 were unchanged in the heart of PPARβ mutants compared to wt (Fig. 8B). Thus,

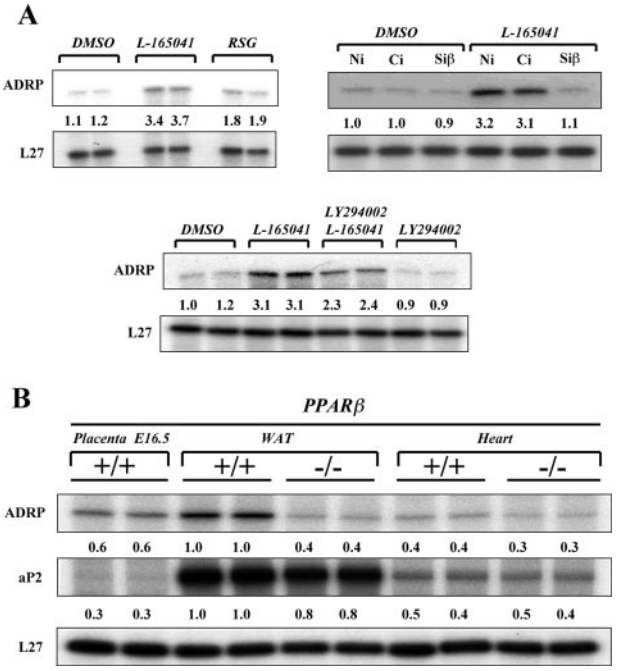

FIG. 8. ADRP expression is associated to giant cell differentiation. (A) Expression profile of ADRP in Rcho-1 cells after 4 days of treatment with L-165041 (5 μM), RSG (1 μM), or PI3K inhibitor (LY294002) (10 μM) (left and bottom panels) and in cells either noninfected (Ni), transduced with the LV-TH (Ci), or transduced with the LV-THsiPPARβ (Siβ) (right panel). Dimethyl sulfoxide (DMSO) was used as a vehicle. (B) Relative mRNA expression profiles of ADRP and aP2 in mouse placental tissues at E16.5, in white adipose tissue (WAT), and in heart. L27 ribosomal protein mRNA was used for normalization. Numbers represent the relative increase (*n*-fold) with respect to basal level in the presence of dimethyl sulfoxide (0.05%) (A) or to level in white adipose tissue (B).

ADRP expression is dependent on PPARβ in some tissues, and most remarkably in the E9.5 placenta giant cells.

In summary, our observations demonstrate the crucial role of PPARβ in the differentiation of the trophoblastic giant cell layer via two overlapping molecular mechanisms which involve a PPARβ-mediated increased Akt1 activity and a direct positive regulation of the transcription factor I-mfa. We further demonstrated that giant cells accumulate lipid, together with the expression of the ADRP protein, conferring on the giant cells an unexpected role in lipid metabolism.

DISCUSSION

The analysis of PPARβ functions in the mouse placenta provides important information. First, although PPARβ and PPARγ are expressed in the three layers of the developing placenta, functional redundancies or compensations between them, if any, are not fully operative. Second, PPARβ is a major regulator of the differentiation of the secondary giant cells, which play a critical role in the establishment of the placental structure and fulfill an important endocrine function. Third, we reveal that secondary giant cells are the prime site of lipid accumulation in the developing placenta, an event which is also under the control of PPARβ.

PPARβ and embryonic lethality. Conflicting results concerning the embryonic lethality of PPARβ null mutant mice appeared in two previous reports (51, 2). Indeed, Peters et al. (51) observed no embryonic lethality on a pure C57BL/6N background but a lower than expected number of newborn homozygous pups on a mixed genetic background. In contrast, Barak et al. (2) reported a severe embryonic lethality in either Sv129 or C57BL/6J background. Our observations are closer to those of Barak et al. (2), with a frequent embryonic lethality between E9.5 and E10.5 due to an altered placenta formation. An explanation of these discrepancies may lie in the mutation performed on the PPARβ gene, with a disruption of the DNA-binding domain therein, as in Barak et al. (2), whereas the mutation performed by Peters et al. (51) disrupted the last 60 amino acids of the ligand-binding domain. The latter approach might have resulted in a hypomorph allele, retaining some aporeceptor functions. A comparative analysis of these two models of PPARβ disruption in a congenic background might reveal very interesting features of PPARβ functions.

The fact that we were able to obtain some productive homozygous pairs, in which the defects in the placenta were still present but less penetrant, is likely due to the presence of one or more modifiers responsible for the higher survival rate of PPARβ$^{-/-}$ embryos. However, while we have not been able so far to improve the survival rate by enriching the mixed genetic background toward Sv129 or toward C57BL/6 background, a contribution of the genetic background to the observed phenotypes cannot be excluded. Large-scale and in-depth genetic studies will be needed to identify the genes that are partners in this complex trait.

PPARβ promotes giant cell differentiation. We demonstrate that deletion of PPARβ leads to a dramatic decrease of the trophoblast secondary giant cell layer in vivo and abolishes the ability of Rcho-1 cells to differentiate into giant cells in cell culture. Conversely, agonist activation of PPARβ in a cell culture model of trophoblast giant cell differentiation markedly accelerates and increases the extent of differentiation.

Our studies contribute to identifying the factors involved in the development and endocrine functions of the placenta. Members of the bHLH factor family are involved in the control of commitment, differentiation, and development of many different tissues and organs, including the placenta (23). Hand1 promotes the differentiation of trophoblast giant cells (53). In contrast, Mash-2 has the opposite effect as it is required to maintain the pool of precursors in the ectoplacental cone and spongiotrophoblast, and its sustained expression precludes their differentiation in giant cells (23). Id-2 belongs to a subset of HLH proteins and acts as a dominant negative factor by dimerizing and sequestering the heterodimerization partner of bHLH transcription factors (48). In Rcho-1 cells, overexpression of a related protein (Id-1) inhibits their differentiation into giant cells (8). This can be paralleled with the expression of Id-2, which is undetectable in differentiated trophoblast giant cells but remains expressed in the extra-embryonic ectoderm of the chorion (30). Finally, the bHLH-repressor protein I-mfa is also required for the generation of trophoblast giant cells, possibly acting as a direct inhibitor of the activity of Mash-2 by preventing its nuclear import (36). In the present study, we demonstrate that PPARβ activation does not affect Hand1 expression but increases I-mfa mRNA levels in a PI3K-independent manner and decreases Id-2 expression in a PI3K-dependent manner. As proposed in Fig. 9 and its legend, these two likely independent mechanisms are converging in trophoblast cell differentiation. Interestingly, the I-mfa mutants exhibit a generally similar phenotype to that of PPARβ mutant embryos, with an overall reduced size of the embryos, a lack of trophoblast giant cells, and a lethality that occurs at mid-gestation (36).

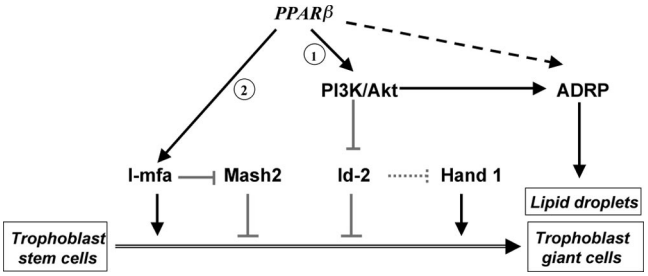

FIG. 9. PPARβ plays a key role in trophoblast giant cell differentiation via two converging mechanisms. Hand1 and Mash-2 are two crucial transcription factors involved in promoting and inhibiting giant cell differentiation, respectively. In addition, Id-2 acts as a dominant negative factor by dimerizing and sequestering the heterodimerization partner of bHLH transcription factors and must be down-regulated to allow trophoblast giant cell differentiation. PPARβ first acts by increasing Akt activity, which leads to Id-2 down-regulation. The bHLH transcription factor targeted by Id-2 in the trophoblast cells is not ascertained but could include Hand1 (dotted line) or the heterodimerization partner of Hand1, which in the giant cells is not yet identified (56). The role of PPARβ in directly regulating Hand1 is unclear since Hand1 expression is not modified in the Rcho-1 cell model. Secondly, PPARβ also increases the expression of I-mfa, which acts as an inhibitor of Mash-2 activity, possibly by impairing its nuclear import. Finally, the subsequent differentiation is associated with ADRP expression and lipid accumulation, which also depends on PPARβ and its activity on Akt-1.

The full activity of PPARβ in promoting giant cell differentiation thus requires an intact PI3K pathway. We previously demonstrated the ability of PPARβ to reinforce Akt signaling upon skin wound healing (11, 12). We now reveal that this activity and regulation by PPARβ are crucial for proper placental development, an observation which parallels the involvement of the PI3K/Akt1 signaling pathway for the development of differentiated trophoblast giant cells (reference 33 and the present study). Our present observations unravel a highly specific pattern of phospho-Akt (P-Akt) in the nucleus of giant cells. Activated Akt can indeed translocate into the nucleus (45). Unfortunately, unlike the known pleiotropic role of P-Akt in the cytoplasm, the role of its nuclear form has yet to be defined. Recent studies using a differentiated thyroid cancer cell line revealed that the ability of the invasive cells to migrate was associated with nuclear localization of P-Akt and that PI3K inhibitors reduced cell motility (60, 34). In the placenta, the association of nuclear P-Akt with trophoblast giant cells suggests a role of P-Akt in giant cell invasiveness. However, the specific events which take place downstream of Akt activity remain to be clarified. Akt has been reported to repress Id-2 expression in neuroblastoma cells (43). In addition, it has been shown to regulate the assembly and activity of bHLH-coactivator complexes in neuronal differentiation (61). Thus, we can propose that the full activity of PPARβ on giant cell

differentiation involves (i) the PI3K-dependent inhibition of Id-2 expression and the up-regulation of the activity of some bHLH factors and (ii) the direct or indirect activation of I-mfa expression (Fig. 9). While a bioinformatic analysis identified a possible PPRE in the I-mfa promoter (data not shown), this DNA element remains to be functionally characterized.

PPARβ and lipid metabolism in the placenta. Our present results strongly support two mechanisms, possibly independent, of lipid storage and ADRP expression in the placenta. At an early stage, when giant cells are forming the main interface between the maternal and the fetal compartments, giant cells are the major site of lipid accumulation, which is accompanied by increased ADRP expression. Herein, we demonstrate that this early ADRP increased expression is PPARβ dependent. At a later stage, upon major development of a functional labyrinth structure, the labyrinth and the maternal decidua become the main sites where lipid droplets are observed, and a careful examination points to the major presence of lipids in the cells that surround the fetal vessels. This labyrinth expression is possibly dependent on PPARγ, as previously suggested (1, 55).

These features are particularly remarkable since both PPARβ and PPARγ are expressed throughout the three placenta layers, suggesting that the specificity of their action must depend on distinct activation processes, including ligand availability and/or target gene specificity. In mice and in humans, ADRP is a known PPAR target gene, and a PPRE identified in the ADRP promoter mediates its response to the PPARβ agonist GW501516 (6, 62) and also to PPARα and to PPARγ (24, 14, 57). In Rcho-1 cells, the full activity of PPARβ to increase the expression of ADRP requires an intact PI3K/Akt1 signaling pathway (Fig. 8) and a successful differentiation in giant cells. Thus, the high level of ADRP mRNA in Rcho-1 differentiated cells is likely the result of two processes: direct transcriptional activity of PPARβ at the ADRP promoter and indirect action of PPARβ on differentiation via the PI3K/Akt1 pathway.

Although elucidation of its function is still in progress, ADRP seems to be involved in the formation and stabilization of lipid droplets (19). Recombinant expression of ADRP in COS-7 cells demonstrated that this protein facilitates the transport of long-chain free fatty acids and may function as a fatty acid carrier protein (18). Our results raise the question as to whether or not lipid accumulation in the giant cells during the early stages of placental development fulfills the same role as it does in the labyrinth cells at a later stage. In the latter, the ADRP location in close proximity to the vessel walls suggests a metabolic role in feto-maternal exchange. This nutritional role in the giant cells cannot be excluded. However, ADRP not only encircles droplets mainly composed of triglycerides, such as those found in the lactating mammary gland, but also droplets rich in cholesterol stored as steroid hormone precursors in adrenocortical cells (27). In the rodent placentas, androgen synthesis takes places within trophoblast giant cells (32). Rcho-1 cells synthesize both progesterone and androstenedione (66). Thus, lipid droplet accumulation and ADRP expression in trophoblast giant cells may rather contribute to the production of steroid hormones. Therefore, PPARβ null concepti would suffer from both a low number of differentiated giant cells and an additional alteration of their endocrine functions via decreased levels of ADRP, consequently impairing placenta and embryonic growth.

In conclusion, we have revealed some crucial regulatory events in giant cell differentiation mediated by PPARβ. These results also bring to light the significant role of PPARβ in correlation with lipid accumulation, which may fulfill an endocrine function as well as contribute to nutrient exchange between the fetus and the mother. Collectively, these observations concerning PPARβ null placentas emphasize the need to carefully evaluate the effects of PPAR ligands on placenta development and physiology when they are considered for use as therapeutic drugs in chronic metabolic diseases, which may also affect pregnant women.

ACKNOWLEDGMENTS

We are grateful to D. Duboule and J. Zakany for help in obtaining the PPARβ mutant mice as well as for stimulating discussion. We also thank D. Metzger and P. Chambon for comments on the manuscript and M. J. Soares for making the Rcho-I cell line available to us. We thank M. Mark for helpful advice, J. Rossant for generous gifts of PL-I and Tpbpa probes, F. Guillemot for providing us with the Mash-2 cDNA, and C. Schneider and D. Galaud for technical assistance.

This work was supported by grants from Swiss National Science Foundation to B.D. and W.W.

REFERENCES

1. **Barak, Y., M. C. Nelson, E. S. Ong, Y. Z. Jones, P. Ruiz-Lozano, K. R. Chien, A. Koder, and R. M. Evans.** 1999. PPAR gamma is required for placental, cardiac, and adipose tissue development. Mol. Cell **4:**585–595.
2. **Barak, Y., D. Liao, W. He, E. S. Ong, M. C. Nelson, J. M. Olefsky, R. Boland, and R. M. Evans.** 2002. Effects of peroxisome proliferator-activated receptor delta on placentation, adiposity, and colorectal cancer. Proc. Natl. Acad. Sci. USA **99:**303–308.
3. **Bedu, E., W. Wahli, and B. Desvergne.** 2005. Peroxisome proliferator-activated receptor beta/delta as a therapeutic target for metabolic diseases. Expert Opin. Ther. Targets **9:**861–873.
4. **Bildirici, I., C. R. Roh, W. T. Schaiff, B. M. Lewkowski, D. M. Nelson, and Y. Sadovsky.** 2003. The lipid droplet-associated protein adipophilin is expressed in human trophoblasts and is regulated by peroxisomal proliferator-activated receptor-gamma/retinoid X receptor. J. Clin. Endocrinol. Metab. **88:**6056–6062.
5. **Braissant, O., F. Foufelle, C. Scotto, M. Dauca, and W. Wahli.** 1996. Differential expression of peroxisome proliferator-activated receptors (PPARs): tissue distribution of PPAR-alpha, -beta, and -gamma in the adult rat. Endocrinology **137:**354–366.
6. **Chawla, A., C. H. Lee, Y. Barak, W. He, J. Rosenfeld, D. Liao, J. Han, H. Kang, and R. M. Evans.** 2003. PPARdelta is a very low-density lipoprotein sensor in macrophages. Proc. Natl. Acad. Sci. USA **100:**1268–1273.
7. **Chen, C. M., N. Kraut, M. Groudine, and H. Weintraub.** 1996. I-mf, a novel myogenic repressor, interacts with members of the MyoD family. Cell **86:**731–741.
8. **Cross, J. C., M. L. Flannery, M. A. Blanar, E. Steingrimsson, N. A. Jenkins, N. G. Copeland, W. J. Rutter, and Z. Werb.** 1995. Hxt encodes a basic helix-loop-helix transcription factor that regulates trophoblast cell development. Development **121:**2513–2523.
9. **Denkins, Y. M., J. Woods, J. E. Whitty, J. H. Hannigan, S. S. Martier, R. J. Sokol, and N. Salem, Jr.** 2000. Effects of gestational alcohol exposure on the fatty acid composition of umbilical cord serum in humans. Am. J. Clin. Nutr. **71:**300S–306S.
10. **Desvergne, B., and W. Wahli.** 1999. Peroxisome proliferator-activated receptors: nuclear control of metabolism. Endocr. Rev. **20:**649–688.
11. **Di Poi, N., N. S. Tan, L. Michalik, W. Wahli, and B. Desvergne.** 2002. Antiapoptotic role of PPARbeta in keratinocytes via transcriptional control of the Akt1 signaling pathway. Mol. Cell **10:**721–733.
12. **Di Poi, N., C. Y. Ng, N. S. Tan, Z. Yang, B. A. Hemmings, B. Desvergne, L. Michalik, and W. Wahli.** 2005. Epithelium-mesenchyme interactions control the activity of peroxisome proliferator-activated receptor β/δ during hair follicle development. Mol. Cell. Biol. **25:**1696–1712.
13. **Doetschman, T. C., H. Eistetter, M. Katz, W. Schmidt, and R. Kemler.** 1985. The in vitro development of blastocyst-derived embryonic stem cell lines: formation of visceral yolk sac, blood islands and myocardium. J. Embryol. Exp. Morphol. **87:**27–45.
14. **Edvardsson, U., A. Ljungberg, D. Linden, L. William-Olsson, H. Peilot-Sjogren, A. Ahnmark, and J. Oscarsson.** 2005. PPARα activation increases

triglyceride mass and adipose differentiation-related protein in hepatocytes. J. Lipid Res.
15. **Faria, T. N., and M. J. Soares.** 1991. Trophoblast cell differentiation: establishment, characterization, and modulation of a rat trophoblast cell line expressing members of the placental prolactin family. Endocrinology **129:** 2895–2906.
16. **Forman, B. M., J. Chen, and R. M. Evans.** 1997. Hypolipidemic drugs, polyunsaturated fatty acids, and eicosanoids are ligands for peroxisome proliferator-activated receptors alpha and delta. Proc. Natl. Acad. Sci. USA **94:**4312–4317.
17. **Fredenrich, A., and P. A. Grimaldi.** 2005. PPAR δ: an uncompletely [sic] known nuclear receptor. Diabetes Metab. **31:**23–27.
18. **Gao, J., and G. Serrero.** 1999. Adipose differentiation related protein (ADRP) expressed in transfected COS-7 cells selectively stimulates long chain fatty acid uptake. J. Biol. Chem. **274:**16825–16830.
19. **Gao, J., H. Ye, and G. Serrero.** 2000. Stimulation of adipose differentiation related protein (ADRP) expression in adipocyte precursors by long-chain fatty acids. J. Cell Physiol. **182:**297–302.
20. **Gardner, R. L., V. E. Papaioannou, and S. C. Barton.** 1973. Origin of the ectoplacental cone and secondary giant cells in mouse blastocysts reconstituted from isolated trophoblast and inner cell mass. J. Embryol. Exp. Morphol. **30:**561–572.
21. **Goberdhan, D. C., and C. Wilson.** 2003. PTEN: tumour suppressor, multifunctional growth regulator and more. Hum. Mol. Genet. **12**(Spec. no. 2)**:** R239–R248.
22. **Guillemot, F., L. C. Lo, J. E. Johnson, A. Auerbach, D. J. Anderson, and A. L. Joyner.** 1993. Mammalian achaete-scute homolog 1 is required for the early development of olfactory and autonomic neurons. Cell **75:**463–476.
23. **Guillemot, F., A. Nagy, A. Auerbach, J. Rossant, and A. L. Joyner.** 1994. Essential role of Mash-2 in extraembryonic development. Nature **371:**333–336.
24. **Gupta, R. A., J. A. Brockman, P. Sarraf, T. M. Willson, and R. N. DuBois.** 2001. Target genes of peroxisome proliferator-activated receptor gamma in colorectal cancer cells. J. Biol. Chem. **276:**29681–29687.
25. **Hamlin, G. P., X. J. Lu, K. F. Roby, and M. J. Soares.** 1994. Recapitulation of the pathway for trophoblast giant cell differentiation in vitro: stage-specific expression of members of the prolactin gene family. Endocrinology **134:** 2390–2396.
26. **Hansen, J. B., H. Zhang, T. H. Rasmussen, R. K. Petersen, E. N. Flindt, and K. Kristiansen.** 2001. Peroxisome proliferator-activated receptor δ (PPARδ)-mediated regulation of preadipocyte proliferation and gene expression is dependent on cAMP signaling. J. Biol. Chem. **276:**3175–3182.
27. **Heid, H. W., R. Moll, I. Schwetlick, H. R. Rackwitz, and T. W. Keenan.** 1998. Adipophilin is a specific marker of lipid accumulation in diverse cell types and diseases. Cell Tissue Res. **294:**309–321.
28. **Hornstra, G., M. D. Al, A. C. van Houwelingen, and M. M. Foreman-van Drongelen.** 1995. Essential fatty acids in pregnancy and early human development. Eur. J. Obstet. Gynecol. Reprod. Biol. **61:**57–62.
29. **Jehl-Pietri, C., C. Bastie, I. Gillot, S. Luquet, and P. A. Grimaldi.** 2000. Peroxisome-proliferator-activated receptor delta mediates the effects of long-chain fatty acids on post-confluent cell proliferation. Biochem. J. **350:** 93–98.
30. **Jen, Y., K. Manova, and R. Benezra.** 1997. Each member of the Id gene family exhibits a unique expression pattern in mouse gastrulation and neurogenesis. Dev. Dyn. **208:**92–106.
31. **Jiang, H. P., and G. Serrero.** 1992. Isolation and characterization of a full-length cDNA coding for an adipose differentiation-related protein. Proc. Natl. Acad. Sci. USA **89:**7856–7860.
32. **Johnson, D. C.** 1992. Cellular localization and factors controlling rat placental cytochrome P45017 alpha (CYP17): 17 alpha-hydroxylase/C17,20-lyase activity. Biol. Reprod. **46:**30–38.
33. **Kamei, T., S. R. Jones, B. M. Chapman, K. L. MCGonigle, G. Dai, and M. J. Soares.** 2002. The phosphatidylinositol 3-kinase/Akt signaling pathway modulates the endocrine differentiation of trophoblast cells. Mol. Endocrinol. **16:**1469–1481.
34. **Kim, C. S., V. V. Vasko, Y. Kato, M. Kruhlak, M. Saji, S. Y. Cheng, and M. D. Ringel.** 2005. Akt activation promotes metastasis in a mouse model of follicular thyroid carcinoma. Endocrinology **146:**4456–4463.
35. **Kliewer, S. A., S. S. Sundseth, S. A. Jones, P. J. Brown, G. B. Wisely, C. S. Koble, P. Devchand, W. Wahli, T. M. Willson, J. M. Lenhard, and J. M. Lehmann.** 1997. Fatty acids and eicosanoids regulate gene expression through direct interactions with peroxisome proliferator-activated receptors alpha and gamma. Proc. Natl. Acad. Sci. USA **94:**4318–4323.
36. **Kraut, N., L. Snider, C. M. Chen, S. J. Tapscott, and M. Groudine.** 1998. Requirement of the mouse I-mfa gene for placental development and skeletal patterning. EMBO J. **17:**6276–6288.
37. **Krey, G., O. Braissant, F. L'Horset, E. Kalkhoven, M. Perroud, M. G. Parker, and W. Wahli.** 1997. Fatty acids, eicosanoids, and hypolipidemic agents identified as ligands of peroxisome proliferator-activated receptors by coactivator-dependent receptor ligand assay. Mol. Endocrinol. **11:**779–791.
38. **Kubota, N., Y. Terauchi, H. Miki, H. Tamemoto, T. Yamauchi, K. Komeda, S. Satoh, R. Nakano, C. Ishii, T. Sugiyama, K. Eto, Y. Tsubamoto, A. Okuno, K. Murakami, H. Sekihara, G. Hasegawa, M. Naito, Y. Toyoshima, S. Tanaka, K. Shiota, T. Kitamura, T. Fujita, O. Ezaki, S. Aizawa, and T. Kadowaki.** 1999. PPAR gamma mediates high-fat diet-induced adipocyte hypertrophy and insulin resistance. Mol. Cell **4:**597–609.
39. **Lemberger, T., B. Staels, R. Saladin, B. Desvergne, J. Auwerx, and W. Wahli.** 1994. Regulation of the peroxisome proliferator-activated receptor alpha gene by glucocorticoids. J. Biol. Chem. **269:**24527–24530.
40. **Lescisin, K. R., S. Varmuza, and J. Rossant.** 1988. Isolation and characterization of a novel trophoblast-specific cDNA in the mouse. Genes Dev. **2:**1639–1646.
41. **Lim, H., R. A. Gupta, W. G. Ma, B. C. Paria, D. E. Moller, J. D. Morrow, R. N. DuBois, J. M. Trzaskos, and S. K. Dey.** 1999. Cyclo-oxygenase-2-derived prostacyclin mediates embryo implantation in the mouse via PPARδ. Genes Dev. **13:**1561–1574.
42. **Lim, H., and S. K. Dey.** 2000. PPAR delta functions as a prostacyclin receptor in blastocyst implantation. Trends Endocrinol. Metab. **11:**137–142.
43. **Lopez-Carballo, G., L. Moreno, S. Masia, P. Perez, and D. Barettino.** 2002. Activation of the phosphatidylinositol 3-kinase/Akt signaling pathway by retinoic acid is required for neural differentiation of SH-SY5Y human neuroblastoma cells. J. Biol. Chem. **277:**25297–25304.
44. **Mano, H., C. Kimura, Y. Fujisawa, T. Kameda, M. Watanabe-Mano, H. Kaneko, T. Kaneda, Y. Hakeda, and M. Kumegawa.** 2000. Cloning and function of rabbit peroxisome proliferator-activated receptor delta/beta in mature osteoclasts. J. Biol. Chem. **275:**8126–8132.
45. **Meier, R., D. R. Alessi, P. Cron, M. Andjelkovic, and B. A. Hemmings.** 1997. Mitogenic activation, phosphorylation, and nuclear translocation of protein kinase Bβ. J. Biol. Chem. **272:**30491–30497.
46. **Michalik, L., B. Desvergne, N. S. Tan, S. Basu-Modak, P. Escher, J. Rieusset, J. M. Peters, G. Kaya, F. J. Gonzalez, J. Zakany, D. Metzger, P. Chambon, D. Duboule, and W. Wahli.** 2001. Impaired skin wound healing in peroxisome proliferator-activated receptor (PPAR)α and PPARβ mutant mice. J. Cell Biol. **154:**799–814.
47. **Nieder, G. L., and L. Jennes.** 1990. Production of mouse placental lactogen-I by trophoblast giant cells in utero and in vitro. Endocrinology **126:**2809–2814.
48. **Norton, J. D., R. W. Deed, G. Craggs, and F. Sablitzky.** 1998. Id helix-loop-helix proteins in cell growth and differentiation. Trends Cell Biol. **8:**58–65.
49. **Ogren, L., and F. Talamantes.** 1988. Prolactins of pregnancy and their cellular source. Int. Rev. Cytol. **112:**1–65.
50. **Oliver, W. R., Jr., J. L. Shenk, M. R. Snaith, C. S. Russell, K. D. Plunket, N. L. Bodkin, M. C. Lewis, D. A. Winegar, M. L. Sznaidman, M. H. Lambert, H. E. Xu, D. D. Sternbach, S. A. Kliewer, B. C. Hansen, and T. M. Willson.** 2001. A selective peroxisome proliferator-activated receptor delta agonist promotes reverse cholesterol transport. Proc. Natl. Acad. Sci. USA **98:**5306–5311.
51. **Peters, J. M., S. S. Lee, W. Li, J. M. Ward, O. Gavrilova, C. Everett, M. L. Reitman, L. D. Hudson, and F. J. Gonzalez.** 2000. Growth, adipose, brain, and skin alterations resulting from targeted disruption of the mouse peroxisome proliferator-activated receptor β(δ). Mol. Cell. Biol. **20:**5119–5128.
52. **Rieusset, J., J. Seydoux, S. I. Anghel, P. Escher, L. Michalik, T. N. Soon, D. Metzger, P. Chambon, W. Wahli, and B. Desvergne.** 2004. Altered growth in male peroxisome proliferator-activated receptor gamma (PPARγ) heterozygous mice: involvement of PPARγ in a negative feedback regulation of growth hormone action. Mol. Endocrinol. **18:**2363–2377.
53. **Riley, P., L. Anson-Cartwright, and J. C. Cross.** 1998. The Hand1 bHLH transcription factor is essential for placentation and cardiac morphogenesis. Nat. Genet. **18:**271–275.
54. **Ruffner, H., L. F. Reis, D. Naf, and C. Weissmann.** 1993. Induction of type I interferon genes and interferon-inducible genes in embryonal stem cells devoid of interferon regulatory factor 1. Proc. Natl. Acad. Sci. USA **90:** 11503–11507.
55. **Sapin, V., P. Dolle, C. Hindelang, P. Kastner, and P. Chambon.** 1997. Defects of the chorioallantoic placenta in mouse RXRα null fetuses. Dev. Biol. **191:**29–41.
56. **Scott, I. C., L. Anson-Cartwright, P. Riley, D. Reda, and J. C. Cross.** 2000. The HAND1 basic helix-loop-helix transcription factor regulates trophoblast differentiation via multiple mechanisms. Mol. Cell. Biol. **20:**530–541.
57. **Tachibana, K., Y. Kobayashi, T. Tanaka, M. Tagami, A. Sugiyama, T. Katayama, C. Ueda, D. Yamasaki, K. Ishimoto, M. Sumitomo, Y. Uchiyama, T. Kohro, J. Sakai, T. Hamakubo, T. Kodama, and T. Doi.** 2005. Gene expression profiling of potential peroxisome proliferator-activated receptor (PPAR) target genes in human hepatoblastoma cell lines inducibly expressing different PPAR isoforms. Nucl. Recept. **3:**3. [Online.] doi:10.1186/1478-1336-3-3.
58. **Tan, N. S., L. Michalik, N. Noy, R. Yasmin, C. Pacot, M. Heim, B. Fluhmann, B. Desvergne, and W. Wahli.** 2001. Critical roles of PPAR beta/delta in keratinocyte response to inflammation. Genes Dev. **15:**3263–3277.
59. **van der Hoeven, F., J. Zakany, and D. Duboule.** 1996. Gene transpositions in the HoxD complex reveal a hierarchy of regulatory controls. Cell **85:**1025–1035.
60. **Vasko, V., M. Saji, E. Hardy, M. Kruhlak, A. Larin, V. Savchenko, M. Miyakawa, O. Isozaki, H. Murakami, T. Tsushima, K. D. Burman, C. De**

Micco, and M. D. Ringel. 2004. Akt activation and localisation correlate with tumour invasion and oncogene expression in thyroid cancer. J. Med. Genet. **41:**161–170.

61. **Vojtek, A. B., J. Taylor, S. L. DeRuiter, J. Y. Yu, C. Figueroa, R. P. Kwok, and D. L. Turner.** 2003. Akt regulates basic helix-loop-helix transcription factor-coactivator complex formation and activity during neuronal differentiation. Mol. Cell. Biol. **23:**4417–4427.
62. **Vosper, H., L. Patel, T. L. Graham, G. A. Khoudoli, A. Hill, C. H. Macphee, I. Pinto, S. A. Smith, K. E. Suckling, C. R. Wolf, and C. N. Palmer.** 2001. The peroxisome proliferator-activated receptor delta promotes lipid accumulation in human macrophages. J. Biol. Chem. **276:**44258–44265.
63. **Wang, Y. X., C. L. Zhang, R. T. Yu, H. K. Cho, M. C. Nelson, C. R. Bayuga-Ocampo, J. Ham, H. Kang, and R. M. Evans.** 2004. Regulation of muscle fiber type and running endurance by PPARδ. PLOS Biol. **2:**e294.
64. **Willson, T. M., P. J. Brown, D. D. Sternbach, and B. R. Henke.** 2000. The PPARs: from orphan receptors to drug discovery. J. Med. Chem. **43:**527–550.
65. **Wiznerowicz, M., and D. Trono.** 2003. Conditional suppression of cellular genes: lentivirus vector-mediated drug-inducible RNA interference. J. Virol. **77:**8957–8961.
66. **Yamamoto, T., B. M. Chapman, D. C. Johnson, C. R. Givens, S. H. Mellon, and M. J. Soares.** 1996. Cytochrome P450 17 alpha-hydroxylase gene expression in differentiating rat trophoblast cells. J. Endocrinol. **150:**161–168.
67. **Yang, Z. Z., O. Tschopp, M. Hemmings-Mieszczak, J. Feng, D. Brodbeck, E. Perentes, and B. A. Hemmings.** 2003. Protein kinase B alpha/Akt1 regulates placental development and fetal growth. J. Biol. Chem. **278:**32124–32131.